Mercury mobilization and episodic stream acidification during snowmelt: Role of hydrologic flow paths, source areas, and supply of dissolved organic carbon

Jason D. Demers,[1,2] Charles T. Driscoll,[3] and James B. Shanley[4]

Received 22 March 2008; revised 29 July 2009; accepted 9 September 2009; published 27 January 2010.

[1] We quantified hydrologic source areas and flow paths, acid-base and aluminum chemistry, dissolved organic carbon dynamics, and mercury mobilization during snowmelt at the Hubbard Brook Experimental Forest (HBEF), New Hampshire, USA. Here we show (1) episodic acidification during snowmelt at the HBEF is controlled by multiple mechanisms (base cation dilution, nitrate and aluminum acidity, and natural organic acids) and persists despite long-term decreases in acidic deposition; (2) episodic acidification continues to result in mobilization of inorganic monomeric aluminum to concentrations toxic to fish; (3) DOC mobilized from shallow organic soils during snowmelt results in the mobilization of mercury from these same sources; (4) methyl mercury may be produced in the forest floor over winter and flushed from soils during snowmelt; (5) the amount of mercury released during snowmelt likely represents a large portion of annual mercury export; and (6) hydrologic source areas and flow paths, as well as DOC dynamics, strongly influence episodic acidification and the mobilization of mercury, even in a watershed with low stream water DOC concentrations and export.

Citation: Demers, J. D., C. T. Driscoll, and J. B. Shanley (2010), Mercury mobilization and episodic stream acidification during snowmelt: Role of hydrologic flow paths, source areas, and supply of dissolved organic carbon, *Water Resour. Res.*, *46*, W01511, doi:10.1029/2008WR007021.

1. Introduction

[2] Environmental perturbations such as acid and mercury deposition do not occur in isolation, and ecosystem recovery from such perturbations will likely have some degree of interdependence. Hydrological processes and dissolved organic carbon (DOC) dynamics that link terrestrial and aquatic ecosystems are, in part, drivers of episodic acidification, aluminum mobilization, and mercury transport from terrestrial to aquatic ecosystems. Although previous stream research has demonstrated a strong relationship between mercury concentration and discharge [e.g., *Schuster et al.*, 2008; *Balogh et al.*, 2006; *Shanley et al.*, 2005, 2002; *Babiarz et al.*, 1998; *Scherbatskoy et al.*, 1998; *Bishop et al.*, 1995], and between mercury and water column carbon (i.e., POC and DOC) [e.g., *Meili*, 1991; *Mierle and Ingram*, 1991; *Shanley et al.*, 2002; *Kolka et al.*, 2001], no previous studies have made detailed multisolute observations of acid-base and aluminum chemistry in conjunction with mercury species across event hydrographs. By quantifying mercury mobilization within the context of episodic acidification, the objective of this study was to improve understanding of hydrologic and biogeochemical controls governing mercury transport from terrestrial to aquatic ecosystems.

[3] Terrestrial ecosystems mediate the transport of atmospheric deposition to and thus the ultimate effects of atmospheric deposition on surface waters. The degree to which acid deposition acidifies surface waters is a function of watershed characteristics, including elevation, forest type, bedrock, soil depth, base saturation, and hydrologic flow paths [e.g., *Lovett et al.*, 1996; *Schaefer et al.*, 1990; *Driscoll et al.*, 1987; *Newton et al.*, 1987; *Chen et al.*, 1984]. Acidification of these drainage waters, in turn, facilitates the export of labile (inorganic) monomeric aluminum (Al_i [*Driscoll and Postek*, 1995; *Driscoll et al.*, 1985; *Johnson et al.*, 1981]). Watersheds additionally mediate surface water acidification and aluminum mobilization through the supply of natural organic solutes (i.e., dissolved organic carbon, DOC) [*Driscoll et al.*, 1994; *Cirmo and Driscoll*, 1993; *Driscoll et al.*, 1989, 1988]. Thus, the mode and magnitude of surface water acidification and aluminum mobilization is a function of both atmospheric deposition, and the hydrological and biogeochemical processes characteristic of individual watersheds.

[4] Similarly, terrestrial ecosystems also mediate the transport of mercury, influencing the amount, timing, and chemical form that is ultimately delivered to aquatic ecosystems. Watershed characteristics affect the amount of mercury deposited to the landscape as well as the form of mercury that is delivered to surface waters. In general, forests enhance mercury deposition to terrestrial ecosystems [*St. Louis et al.*, 2001; *Rea et al.*, 2002], and there is

[1]Department of Natural Resources, Cornell University, Ithaca, New York, USA.
[2]Now at Department of Geological Sciences, University of Michigan, Ann Arbor, Michigan, USA.
[3]Department of Civil and Environmental Engineering, Syracuse University, Syracuse, New York, USA.
[4]U.S. Geological Survey, Montpelier, Vermont, USA.

0043-1397/10/2008WR007021$09.00

some evidence that forest type influences the magnitude and form of mercury deposited [*Demers et al.*, 2007; *Miller et al.*, 2005]. Despite enhanced deposition of mercury, upland forest watersheds generally exhibit lower export of mercury than agricultural and wetland dominated watersheds, due to lower particulate mercury losses in comparison to agricultural ecosystems and lower dissolved mercury losses in comparison to wetland ecosystems. The strong retention of mercury in soils of upland ecosystems is linked to organic matter [*Grigal*, 2002, 2003; *Yin et al.*, 1997; *Meili*, 1991], likely associated with reduced sulfur and nitrogen groups (i.e., thiols and amines [*Khwaja et al.*, 2006; *Drexel et al.*, 2002; *Skyllberg et al.*, 2000]). Subsequent mobilization of mercury is dependent upon decomposition and erosional processes that release dissolved and particulate organic matter. Wetlands also influence the form of mercury released to surface waters, and the amount of methyl mercury in fish has been correlated with the percentage of wetlands within the entire watershed [*Driscoll et al.*, 1995], as ionic mercury is transformed to methyl mercury within anoxic wetland soils [*Branfireun et al.*, 1998; *St. Louis et al.*, 1996]. Thus, the magnitude and form of mercury mobilized from the terrestrial ecosystem to surface waters is also a function of both the atmospheric deposition, and the hydrological and biogeochemical processes as influenced by watershed characteristics.

[5] Terrestrial ecosystems that have been previously impacted by acid deposition may subsequently limit recovery of affected aquatic ecosystems following reductions in inputs. Recovery of acid-impacted watersheds is dependent upon not only reductions in acidic deposition, but also the rate of chemical weathering that will resupply base cations leached during soil acidification and the net loss of sulfur stored from a legacy of elevated atmospheric sulfur deposition [*Driscoll et al.*, 2001]. Recovery of surface waters (and associated fisheries) from mercury contamination is, in part, dependent upon the rate at which mercury is transferred from the uplands to downstream aquatic ecosystems; that is, the residence time of mercury in the terrestrial soil environment. Because mercury transport has been linked to DOC transport, changes in the mobilization of DOC that may occur in concert with environmental change or recovery from acidification may significantly affect mercury transport. In order to predict the recovery of surface waters from elevated atmospheric acid and mercury deposition (e.g., acidification and associated aluminum toxicity, mercury contamination), it is imperative that we not only understand the biogeochemical processes and hydrologic connectivity governing chemical transfer between terrestrial and aquatic ecosystems, but also how recovery from environmental perturbations may be linked through those biogeochemical processes and hydrologic controls.

[6] Hydrologic connectivity between uplands and surface waters is dynamic, with changes in hydrologic flow paths being driven by storm events and seasonal fluctuations. As water tables rise, longer flow paths through deeper terrestrial soils can be short-circuited [e.g., *Dittman et al.*, 2007; *Chen et al.*, 1984]. At sites where the rate of infiltration is high (as at the HBEF [*Pierce*, 1967]) hydrologic events may result in shallow lateral flow through organic rich soils, thus promoting the transport of DOC to surface waters. In the absence of lateral flow, soil solutions migrate vertically through the soil profile, resulting in podzolization, as aluminum and iron are leached from upper mineral horizons and immobilized in lower mineral horizons by organic acids derived from leaf litter and the forest floor [*Driscoll and Postek*, 1995; *De Coninck*, 1980]. Thus, as flow paths and source areas shift in response to hydrologic events, a corresponding shift occurs in the composition of soil solutions contributed to surface waters.

[7] Despite changes in flow paths during high-flow events, *Likens and Bormann* [1995] show that the concentrations of many chemical components change little with increases in discharge at the Hubbard Brook Experimental Forest. In contrast, the concentration-discharge relationships for TSS, DOC, and mercury are more dynamic at the HBEF and at other sites [e.g., *Shanley et al.*, 2002; *Scherbatskoy et al.*, 1998; *Bishop et al.*, 1995; *Likens and Bormann*, 1995] and result in an exponential increase in total flux as concentration increases with increasing discharge. In dilute systems, even small changes in concentration-discharge dynamics can have important implications, especially where ecological effects may be threshold-dependent. For example, high nitrate pulses during snowmelt can have deleterious effects on the water quality of downstream ecosystems [e.g., *Sullivan et al.*, 1997; *Schaefer et al.*, 1990; *Driscoll et al.*, 1987; *Driscoll and Schafran*, 1984], and associated increases of labile (inorganic) monomeric aluminum may be harmful to aquatic biota if toxic thresholds are exceeded [e.g., *Baker et al.*, 1996; *Van Sickle et al.*, 1996; *Gagen et al.*, 1993, 1994; *Baker and Schofield*, 1982]. Thus, knowledge of both the total annual load and the timing and distribution of the delivery of those loads from uplands to surface waters is important in assessing the recovery of aquatic ecosystems in response to decreases in the deposition of atmospheric pollutants to terrestrial watersheds.

[8] High-flow events are also important to the transfer of mercury from watersheds to surface waters [*Schuster et al.*, 2008; *Shanley et al.*, 2002; *Scherbatskoy et al.*, 1998], and the quantity and form of mercury flux during high-flow events is dependent upon watershed characteristics [e.g., *Babiarz et al.*, 1998; *Hurley et al.*, 1998, 1995; *Bishop et al.*, 1995]. Recent evidence suggests that mercury retention within terrestrial ecosystems of the midwestern and northeastern United States and Canada has declined from about 95% to 78% of annually deposited mercury [*Engstrom and Swain*, 1997; *Lorey and Driscoll*, 1999; *Kamman and Engstrom*, 2002]. However, there is currently a lack in understanding of the mechanisms that govern the release of mercury from terrestrial soils [*Munthe et al.*, 2007]. Hence, although it is important to constrain current estimates of mercury flux from the terrestrial landscape, we must also strive for a mechanistic understanding of the hydrological and biogeochemical processes governing the transfer of mercury from soils to surface waters.

[9] In this study we use base flow and soil solution chemistry as end-members from which to model event flow paths and contributing source areas during snowmelt in the reference watershed (W6) at the Hubbard Brook Experimental Forest. We provide detailed observations of acid-base and aluminum chemistry, DOC dynamics, and mercury mobilization across the snowmelt hydrograph. Based on our observations of acid-base chemistry, DOC dynamics, and modeled hydrologic flow paths, we infer source and process

level controls on mercury mobilization. Here we show that the dynamics of episodic acidification, aluminum mobilization, and mercury transport are linked through hydrological and biogeochemical processes that influence the source and character of the DOC supply from terrestrial to aquatic ecosystems.

2. Methods

2.1. Site Description

[10] In this study we quantify soil solution and stream chemistry in watershed 6 (W6) at the Hubbard Brook Experimental Forest (HBEF) in the southern White Mountains of New Hampshire, USA (43°56′N, 71°45′W). Watershed 6 (W6), the biogeochemical reference watershed at the HBEF, is 13.2 ha in area, located on the south facing slope (mean slope 15.8°, aspect S32°E), has an elevation ranging from ∼540 m at the weir to ∼800 m on the ridge, and is gauged with a modified San Dimas flume (*Likens and Bormann* [1995] and www.hubbardbrook.org).

[11] The climate of the HBEF is humid continental, with short, cool summers and long, cold winters [*Likens and Bormann*, 1995]. Average daily mean temperature (1956–2000) is 5.6°C, with mean monthly temperature increasing to 18.7°C in July, and decreasing to −8.3°C in January [*Bailey et al.*, 2003]. Average annual precipitation at the HBEF (W6) is ∼1,400 mm [*Bailey et al.*, 2003], with ∼30% delivered as snow [*Likens and Bormann*, 1995]. A snowpack develops and usually persists from mid-December through mid-April. At an elevation of ∼560 m (reflecting low- to middle-elevation hardwoods on the south facing slope), peak snow depth (∼1.0–1.5 m) occurs in March, and has a snow water equivalent (SWE) of ∼200 mm [*Bailey et al.*, 2003]. As a result of this snowpack, forest soils usually remain unfrozen throughout the winter [*Likens and Bormann*, 1995]. Annual estimated evapotranspiration is ∼500 mm [*Bailey et al.*, 2003]. Precipitation is distributed evenly throughout the year, whereas approximately one third of total streamflow occurs during the snowmelt period (late March through early May). Soils at the HBEF are well-drained Spodosols, predominantly Haplorthods of sandy loam texture [*Johnson et al.*, 2000; *Likens and Bormann*, 1995]. Precipitation (and snowmelt) infiltrates the soil rapidly, resulting in negligible overland flow [*Detty*, 2008; *Pierce*, 1967].

[12] Stream chemistry at the weir during snowmelt was interpreted within the context of soil solutions and longitudinal stream samples taken from W6 on 28 April 2005. This snapshot characterization of acid-base chemistry and DOC dynamics along this elevational gradient is part of monthly monitoring ongoing at the HBEF since ∼1984 [*Johnson et al.*, 2000]. Watershed 6 was initially divided into three subcatchments of roughly equal area based on elevation and topography (Figure 1); subsequently, W6 was divided into vegetation zones. The uppermost subcatchment (∼710–800 m) represents ∼41% (5.4 ha) of the watershed (as calculated from grid map data at www.hubbardbrook.org). Within the uppermost elevational subcatchment, the spruce-fir-birch (SFB) and the high-elevation hardwoods (HH) are the dominant vegetation zones. The dominant vegetation in the SFB zone includes red spruce (*Picea rubens* Sarg.), balsam fir (*Abies balsamea* L.), and white birch (*Betula papyrifera* var. *cordifolia* Marsh.). The SFB zone (1.6 ha, ∼12% of total catchment area) occurs along the ridge in the northeastern corner of the watershed, where the topography is relatively flat, soils and till are shallow, and some bedrock is exposed. Soils in the SFB zone have a thick O horizon (∼8.9 cm) and an average total depth of 42.8 cm to C horizon or bedrock [*Johnson et al.*, 2000]. The high hardwood zone (HH, 3.4 ha, ∼26% of total catchment area) covers most of the rest of the upper subcatchment, and is dominated by American beech (*Fagus grandifolia* Ehrh.), yellow birch (*Betula allegheniensis* Britt.), and sugar maple (*Acer saccharum* Marsh.). Soils in the high hardwoods are generally deeper (∼6.0 cm O horizon, ∼64.5 cm total depth) but often lie directly on bedrock with no C horizon present [*Johnson et al.*, 2000]. The middle subcatchment (∼625 m to 710 m, 4.5 ha) is mostly dominated by sugar maple and beech. The lower subcatchment (∼540 m to 625 m, 3.1 ha) is a more equal mix of sugar maple, beech, and yellow birch. Together, the middle and lower subcatchments are collectively studied as the low hardwoods zone (LH, 7.9 ha, ∼60% of total catchment area). The soils in the LH zone are deeper, and underlain by dense glacial till (∼6.4 cm O horizon, ∼60.5 cm total depth to C horizon), and the stream flows continuously at this elevation except in times of drought [*Johnson et al.*, 2000].

2.2. Sampling Procedures

[13] Stream samples obtained to characterize stream water chemistry across the snowmelt hydrograph were taken just above the weir in W6. Samples for mercury analyses were collected in new 2 L PETG bottles, using clean procedures [*United States Environmental Protection Agency*, 1996]. Samples for analysis of dissolved organic carbon (DOC) and total suspended solids (TSS) were collected in clean, oven-baked 1 L amber glass bottles. Stream water for the remaining chemical analyses was collected in polyethylene bottles and filled to minimize headspace. Samples were kept cold and in the dark until sample filtering and preservation (i.e., within 48 h of sampling).

[14] Soil solutions were collected during the snowmelt period from tension-free lysimeters installed in the Oa, Bh and Bs soil horizons at 3 sites adjacent to W6 at elevations of 750 m (SFB zone), 730 m (HH zone), and 600 m (LH zone). Additional information about lysimeter placement, construction, and installation is available (*Johnson et al.* [2000], *Dahlgren and Driscoll* [1994], *Driscoll et al.* [1988], and online at www.hubbardbrook.org).

[15] Longitudinal stream samples were collected from 6 sites spaced along an elevational gradient between the stream origin and the weir in W6 (Figure 1), and were collected in conjunction with soil solutions. Stream sites 1 and 2 primarily drain the SFB zone, sites 3 and 4 primarily drain the SFB and HH zones, and sites 5 and 7 drain the combined SFB, HH, and LH zones (there is no site 6 [*Palmer et al.*, 2004]). Snow depth and snow water equivalent (SWE) were measured weekly at elevations of 560 m and 760 m on the south facing slope at the HBEF, and reflect snow conditions at low- to middle-elevation hardwood forests and high-elevation hardwood forests, respectively [*Bailey et al.*, 2003; A. S. Bailey, Snow Depth and Snow Water Data, 2005, available at www.hubbardbrook.org, hereafter Bailey, 2005].

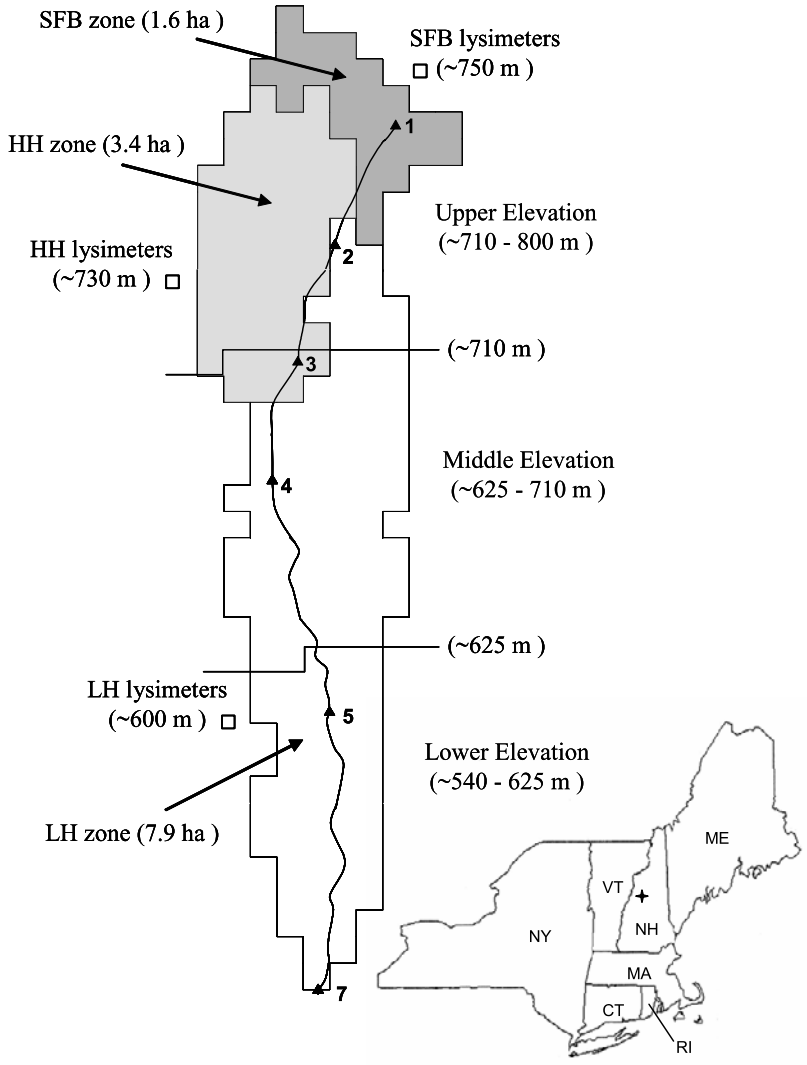

Figure 1. Diagram of watershed 6 at the Hubbard Brook Experimental Forest (HBEF) in the White Mountains of New Hampshire, USA, showing elevational subcatchments and vegetation zones, soil solution lysimeter plots, and longitudinal stream sampling points (adapted from data available online at www.hubbardbrook.org). Elevation at each grid corner available online. Abbreviations are SFB, high-elevation spruce-fir-birch; HH, high-elevation hardwood; LH, low-elevation hardwood. The location of the HBEF is denoted by the cross in the inset map of the northeastern United States.

2.3. Chemical Analyses

[16] Standard procedures were used for the analysis of chemical parameters in stream water. The pH, acid neutralizing capacity (ANC), and dissolved inorganic carbon (DIC) were determined for bulk (unfiltered, unpreserved) samples. Cations, anions, silica, and monomeric aluminum (Al_m) samples were syringe filtered (0.45 μm polypropylene). For TSS, the entire one liter sample was filtered through a preweighed glass fiber filter (0.7 μm, prebaked at 450°C) into a clean flask. The filtrate was then subsampled for analysis of DOC. Samples for analysis of mercury were vacuum filtered through a 0.45 μm Teflon membrane following clean techniques. Both filtered and unfiltered samples were poured into Teflon bottles subsequent to filtering, acidified to 0.4% with hydrochloric acid and stored in the dark at 4°C until analysis. The concentration of total mercury (all forms of mercury) was determined for both unfiltered (Hg_t) and filtered (Hg_d) samples. The concentration of particulate bound mercury was estimated by difference (i.e., $Hg_p = Hg_t - Hg_d$). The concentration of methyl mercury (MeHg) was also determined for both unfiltered (MeHg) and filtered ($MeHg_d$) samples. Methods used for chemical analyses and quality control and quality assurance are described in auxiliary material.[1]

2.4. Acid-Base Calculations

[17] We summarized acid-base chemistry using the following equations; all components are expressed in μeq/L; base cations, metal cations, and inorganic acid

[1] Auxiliary materials are available in the HTML. doi:10.1029/2008WR007021.

anions are denoted by C_B, Me^{n+}, and C_A, respectively (equations (1)–(6)).

$$\text{Cations} = [C_B] + [Me^{n+}] + [H^+] \quad (1)$$

$$[C_B] = [Na^+] + [K^+] + [Mg^{2+}] + [Ca^{2+}] + [NH_4^+] \quad (2)$$

$$[Me^{n+}] = [Al^{3+}] + [Fe^{3+}] + [Mn^{2+}] \quad (3)$$

$$\text{Inorganic Anions} = [C_A] + [HCO_3^-] + [CO_3^{2-}] + [OH^-] \quad (4)$$

$$[C_A] = [NO_3^-] + [SO_4^{2-}] + [Cl^-] + [F^-] \quad (5)$$

$$\text{Calculated Alkalinity} = C_{ALK} = C_B - C_A \quad (6)$$

[18] Organic acid anion $[A^-]$ was determined by charge balance discrepancy [*Driscoll and Newton*, 1985; *Driscoll et al.*, 1989, 1994] (equation (7)). We determined the charge associated with inorganic monomeric aluminum (Al_i) and other metal cations from speciation calculations using the chemical equilibrium model CHEAQS Pro 2007.1 (Chemical Equilibria in Aquatic Systems, Wilko Verweij, available online at http://home.tiscali.nl/cheaqs/index.html). The proportion of strong acids (A_s) and weak acids (A_w) were estimated [*Munson and Gherini*, 1993] (equations (8) and (9)) and organic acid anion charge density was determined by dividing $[A^-]$ (μeq/L) by the concentration of DOC (μmol/L).

$$[A^-] = [C_B] + [Me^{n+}] - [C_A] - [HCO_3^-] + [H^+] \quad (7)$$

$$[A_s] = [C_B] + [Me^{n+}] - [C_A] - [ANC_{gran}] \quad (8)$$

$$[A_w] = [A^-] - [A_s] \quad (9)$$

2.5. Hydrograph Separation

[19] We performed a hydrograph separation for the snowmelt period by utilizing a principal components analysis (PCA) [*McCune and Grace*, 2002] combined with an end-member mixing analysis (EMMA) model following *Christophersen and Hooper* [1992] as well as others [*Burns et al.*, 2001; *Wellington and Driscoll*, 2004]. Procedural details are described in auxiliary material.

3. Results and Discussion

3.1. Snowmelt Hydrograph

[20] Snowmelt associated discharge (~357 mm) from 24 March through 7 May 2005 (DOY 83–127) accounted for ~30.5% of total annual discharge (1172 mm) (J. L. Campbell and A. S. Bailey, Daily Streamflow Data and Daily Precipitation Data, 2005, available at www.hubbardbrook.org, hereafter Campbell and Bailey, 2005). Overall, flow ranged from 1.3 L/s at base flow to 162 L/s during peak flow (Figure 2). Two rain-on-snow events dominated snowmelt discharge, the first on 3 April (71 mm, 162 L/s) likely representing a greater proportion of snowmelt from the lower elevations, and the second on 24 April (62 mm, 122 L/s) likely representing a greater proportion of snowmelt from higher elevations (see section 3.2). These two high-flow events coincided with 51 mm and 106 mm of rainfall, respectively (Figure 2) (Campbell and Bailey, 2005). Maximum snow depth in the low- to middle-elevation hardwoods (at 560 m) was 70.1 cm (SWE = 17.5 cm); this low-elevation zone was snow-free by approximately 11 April. Maximum snow depth in the high hardwoods (at ~760 m) was 93.7 cm (SWE = 23.9 cm); this higher-elevation zone was snow free by approximately 26 April (Bailey, 2005). Snow depth, SWE, timing of snowmelt, the amount of precipitation during snowmelt, and snowmelt runoff were near average relative to the long-term record at the HBEF (Table 1). Sampling coverage included two base flow samples prior to snowmelt (Q = 1.3, 1.4 L/s) and one base flow sample after snowmelt (Q = 3.1 L/s (Figure 2)); the remaining samples were obtained over a range of elevated flows (Q = 5.0 to 93.4 L/s), although the two largest discharge peaks were sampled only on their descending limbs. Overall, the snowmelt period was well characterized by the sampling effort across the hydrograph (Figure 2).

3.2. Hydrograph Separation

[21] A chemical separation of the hydrograph using principal components analysis (PCA) and an end-member mixing analysis (EMMA) model revealed that a large proportion of stream discharge was derived from shallow soil water during the snowmelt period (Figure 2). This model result is in good agreement with previous research within this watershed [*Dittman et al.*, 2007; *Lawrence and Driscoll*, 1990; *McDowell*, 1985]. The first principal component appeared to represent variation between deep soil water and shallow soil water contributions to the stream, whereas the second principal component appeared to represent differences in soil solution chemistry along an elevational gradient within the watershed (Figure 3). The first principal component accounted for 69.7% of the variation in solute chemistry, whereas the second principal component accounted for an additional 19.0%, together explaining 88.7% of the variation in the model. Note that most studies differentiate source water contributions along a vertical gradient within the soil profile (i.e., principal component axis one) [e.g., *Christophersen and Hooper*, 1992; *Wellington and Driscoll*, 2004], whereas few separate sources among geographically distinct areas [*Burns et al.*, 2001] or consider an elevational gradient of subcatchments [e.g., *Johnson et al.*, 2000; *Lawrence and Driscoll*, 1990; *Driscoll et al.*, 1988]. Conceptually, this reflects that subcatchment contributions to total watershed discharge are often approximated using relative watershed area. However, as subcatchments have differing amounts of accumulated snow and differ in their timing and rate of snowmelt along the elevational gradient, it is reasonable to expect that the relative contribution of each subcatchment along an elevational gradient might shift as the snowmelt period proceeds. Moreover, *Lawrence and Driscoll* [1990] showed that contributions from subcatchments along an elevational

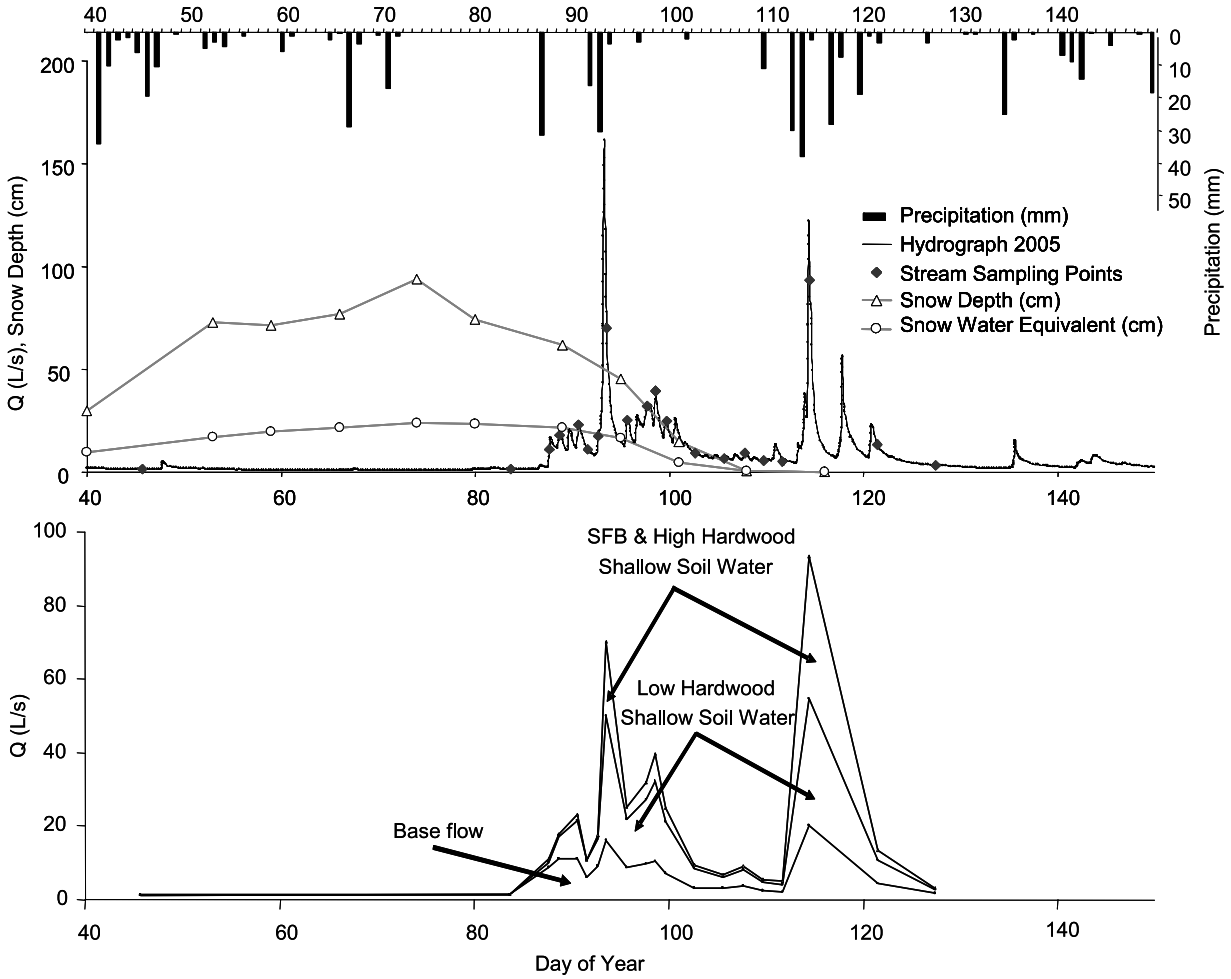

Figure 2. Snowpack, precipitation, discharge, and hydrograph separation based on PCA-EMMA model during snowmelt at W6 at the Hubbard Brook Experimental Forest. Base flow represents deep soil water.

Table 1. Maximum Snow Depth, Maximum Snow Water Equivalent, Date of Completion of Snowmelt, Precipitation Occurring During the Snowmelt Period, and Snowmelt Runoff for W6 at the Hubbard Brook Experimental Forest[a]

	Entire Watershed 6	Low-/Middle-Elevation Hardwoods	High-Elevation Hardwoods
		Maximum Snow Depth (mm)	
1985–1994		343–892, 647 (207)	470–1057, 792 (240)
1995–2004		404–886, 633 (148)	599–1176, 833 (198)
2005		701	937
		Maximum SWE (mm)	
1985–1994		89–226, 163 (47)	107–272, 214 (60)
1995–2004		97–249, 160 (54)	122–305, 213 (59)
2005		173	239
		Completion of Melt (DOY)	
1985–1994		78–118, 103 (11)	78–122, 106 (13)
1995–2004		87–119,101 (10)	96–127, 109 (10)
2005		101	116
		Snowmelt Precipitation (mm)	
1985–1994	45–252, 169 (59)		
1995–2004	67–385, 195 (107)		
2005	192		
		Snowmelt Runoff (mm)	
1985–1994	169–363, 278 (65)		
1995–2004	149–448, 293 (102)		
2005	357		

[a]Data are given as range, mean, and +/− 1 standard deviation (values in parentheses) for the 1985–1994 and 1995–2004 periods. For the purposes of this historic context, the snowmelt period was determined to begin at date of maximum snowpack in the low-/middle-elevation hardwoods and end at date of snowpack disappearance in the high-elevation hardwoods. Summary data were compiled from data available online at www.hubbardbrook.org (Bailey, 2005; Campbell and Bailey, 2005).

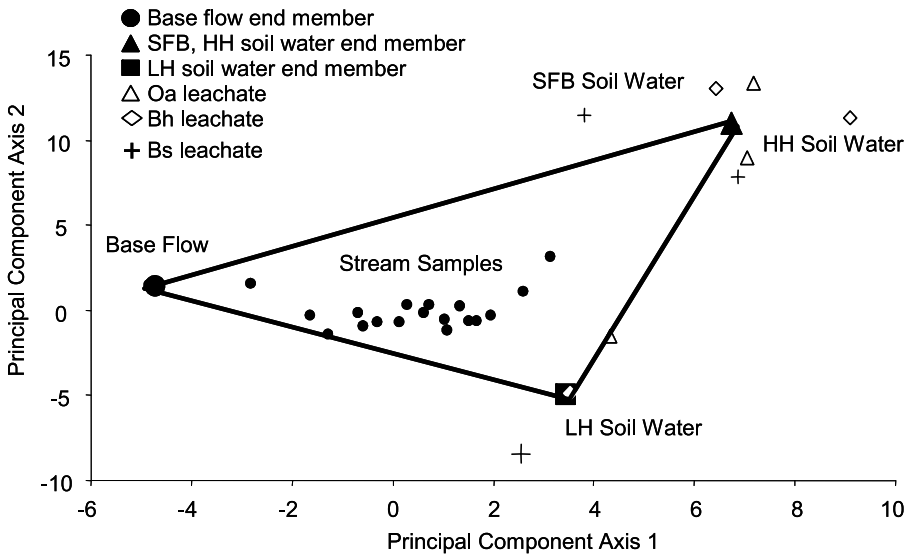

Figure 3. Mixing diagram generated with principal component analysis showing snowmelt stream water scores bounded by deep soil water and shallow soil water end-members. Principal component axis one represents the increasing contribution of shallow soil water as opposed to deep soil water (as represented by base flow); principal component axis two represents soil water contributions from different subcatchments along an elevational gradient within the watershed.

gradient differed in chemical composition. Thus, as the proportions of water originating from individual subcatchments vary, corresponding shifts in stream water chemistry will result.

[22] Snowmelt hydrograph separations have also been performed in other watersheds at the HBEF. *Hooper and Shoemaker* [1986] used stable isotopes of water and dissolved silica to separate old and new water during snowmelt in W3, showing that the discharge was dominated by old water (i.e., water that was present in the watershed prior to snowmelt). *Wellington and Driscoll* [2004] used a PCA-EMMA to separate sources of stream water during snowmelt in W9 (a north facing conifer-dominated watershed), finding that shallow soil water was a dominant source of stream water during high flows. Neither of these previous studies at Hubbard Brook attempted to distinguish geographically distinct source areas within the watershed.

[23] In our study, the PCA-EMMA showed that three distinct soil water end-members bounded the chemical composition of stream water (Figure 3). The deep soil water end-member was represented by preevent stream base flow. Shallow soil water end-members were represented by soil solution from lysimeters in subcatchments along an elevational gradient (Figure 1). The first shallow soil water end-member was represented by the average soil water chemistry from the O_a, B_h, and B_s horizons in the LH subcatchment. Soil solution chemistry from the HH and SFB subcatchments clustered together during PCA, and thus their average solution chemistry was used for the second shallow soil water end-member.

[24] According to the PCA-EMMA model, the contribution of shallow soil water to total stream discharge ranged from 21% at the onset of snowmelt (10.9 L/s) to 78% at the sampled peaks in discharge (93.4 L/s (Figure 2)). An analysis of the elevational component revealed that the contribution of shallow soil water from the HH and SFB subcatchments was more dynamic and occurred later during the snowmelt period (as snowmelt was delayed at elevation), contributing 29% and 42% of stream discharge during the two largest flows measured (Figure 2).

[25] The EMMA model was a reasonably good predictor of stream solute chemistry. Solute chemistry predicted by the model was fairly well correlated with measured stream chemistry (r = 0.90, 0.81, 0.92, 0.85, 0.96, and 0.93 for F^-, SO_4^{2-}, Al_o, Na^+, Mg^{2+} and Ca^{2+}, respectively); however, the slope of the relationship between predicted and measured values varied (0.69, 1.69, 0.85, 2.78, 1.00, and 0.98 for F^-, SO_4^{2-}, Al_o, Na^+, Mg^{2+} and Ca^{2+}, respectively). The slope was closer to unity for Ca and Mg, solutes that were most associated with the first principal component and were expected to behave most conservatively.

[26] Modeled soil water contributions also agreed qualitatively with the observed patterns in soil lysimeter and stream water chemistry not explicitly included in the model. Nitrate is known to peak during snowmelt (as it does in this study), and *Campbell et al.* [2006] used dual isotope analysis to demonstrate that this nitrate originates from shallow soils and has been processed prior to entry into the stream (i.e., nitrate is not directly contributed from meltwater). *Dittman et al.* [2007] also showed that shallow flow short-circuits deeper flow paths at higher elevations during high flow in this watershed. Moreover, soil solutions collected from lysimeters during the snowmelt period represent sources of nitrate and DOC that are available for export through shallow flow paths during high-flow events, and nitrate and DOC concentrations in these soil solutions during snowmelt were high enough to contribute to peak concentrations observed in stream water (Tables 2, 3, and 4). Overall, modeled flow paths demonstrate a spatially and temporally dynamic connectivity between terrestrial and stream ecosystems.

Table 2. Total Concentration of Components During Presnowmelt Base Flow, at Two Peak Flows During Snowmelt, and at Postsnowmelt Base Flow[a]

Component	Presnowmelt Base Flow	Snowmelt		Postsnowmelt Base Flow
		First Peak Flow	Second Peak Flow	
ANCgran	6.2	−1.6 (−7.9)	0.3 (−5.9)	2.5 (−3.8)
C_{ALK}	−7.3	−24.5 (−17.2)	−19.1 (−11.8)	−15.3 (−7.9)
Cations	101.2	101.3 (+0.1)	95.6 (−5.7)	94.8 (−6.5)
C_B	93.1	65.5 (−27.5)	62.2 (−30.9)	74.1 (−19.0)
nMe^{n+}	2.5	21.8 (19.3)	18.7 (16.2)	11.0 (8.5)
Inorganic anions	103.2	91.2 (−12.0)	82.1 (−21.0)	90.7 (−12.4)
C_A	100.4	90.1 (−10.3)	81.3 (−19.2)	89.4 (−11.0)
A^-	−1.9	10.2 (12.1)	13.4 (15.4)	4.1 (6.0)
HCO_3^-	2.7	1.1 (−1.7)	0.9 (−1.9)	1.3 (−1.4)
F^-	1.4	1.6 (0.2)	1.4 (0.0)	1.7 (0.2)
Cl^-	11.0	11.4 (0.5)	10.7 (−0.3)	10.9 (−0.1)
NO_3^-	2.0	15.2 (13.2)	6.0 (4.0)	0.3 (−1.7)
SO_4^{2-}	86.0	61.8 (−24.2)	63.1 (−22.9)	76.6 (−9.5)
Mn^{2+}	0.2	2.8 (2.6)	2.1 (1.9)	0.7 (0.5)
Fe^{n+}	0.0	0.1 (0.1)	0.2 (0.2)	0.1 (0.1)
Al_i^{n+}	2.2	18.8 (16.6)	16.4 (14.2)	9.7 (7.4)
H^+	5.7	14.0 (8.4)	14.7 (9.0)	9.7 (4.0)
NH_4^+	0.3	0.2 (−0.1)	0.7 (0.4)	0.5 (0.2)
K^+	3.9	9.5 (5.6)	8.0 (4.1)	4.8 (1.0)
Na^+	41.9	23.8 (−18.1)	22.9 (−19.0)	33.5 (−8.4)
Mg^{2+}	23.0	13.7 (−9.3)	12.6 (−10.4)	15.1 (−7.9)
Ca^{2+}	24.0	18.4 (−5.6)	18.0 (−6.1)	20.2 (−3.8)

[a]Total concentration of components is in μeq/L. The presnowmelt base flow reference sample was taken 24 March 2005, the first and second peak flow events were sampled on 3 and 24 April 2005, respectively, and postsnowmelt base flow was sampled 7 May 2005. Change in concentration of components (μeq/L) from presnowmelt base flow conditions are shown in parentheses (i.e., Δ values).

3.3. Episodic Acidification

3.3.1. Decreases in ANC and pH

[27] Acid neutralizing capacity (ANC) and pH were lowest during episodes of high stream discharge, with the greatest depression in ANC during discharge peaks at the onset of snowmelt (Figure 4). The pH decreased to 4.85 from a base flow pH of 5.25 during each of the two highest-flow events (Figure 4). ANC decreased by 7.9 μeq/L during the initial high-flow event (3 April, DOY 94) and 5.9 μeq/L during the latter high-flow event (24 April, DOY 115 (Table 2)) to a minimum value of −1.6 μeq/L (Figure 4). These results are in agreement with previous studies of episodic acidification during snowmelt, which have shown that the largest pulses of acidification occur during the first flush of water from shallow soils of acid-impacted forested ecosystems [e.g., *Wigington et al.*, 1996, and references therein].

[28] Multiple mechanisms control episodic acidification during spring snowmelt in lakes and streams of the northeastern United States, driven in part by differences in hydrologic flow paths through the watershed (*Schafran and Driscoll* [1993], *Schaefer et al.* [1990], *Wigington et al.* [1996], and supported by data herein). Depression of ANC and pH in moderate-/high-ANC waters (associated with deep till and deep flow paths) results from meltwater dilution of groundwater-contributed base cations [*Schaefer et al.*, 1990]. Depression of ANC and pH in low-ANC waters (associated with thin tills and shallow flow paths) coincide with pulses of nitrate, aluminum, and associated acidity from the forest floor to the stream during snowmelt [*Schaefer et al.*, 1990]. Sulfate acidity is more important to chronic baseline acidification and nonsnowmelt driven acid episodes [*Wigington et al.*, 1996]. In lakes with ANC near 0 μeq/L (like HBEF stream water), *Schaefer et al.* [1990] showed that both C_B dilution and contributions of nitrate, aluminum, and associated acidity are important drivers of episodic acidification.

[29] In this study, decreases in base cation concentrations in excess of decreases in inorganic strong acid anion concentrations were, in part, responsible for decreases in ANC (i.e., a C_B dilution mechanism (Figure 4)). Overall, base cation patterns resulted from decreases in sodium, magnesium, and calcium ($\Delta Na^+ > \Delta Mg^{2+} > \Delta Ca^{2+}$; K^+ increased (Table 2)). Patterns in total inorganic strong acid anions largely resulted from decreases in sulfate (from 86.0 to 61.8 μeq/L) that were only partially offset by increases in nitrate (from 1.9 to 15.2 μeq/L) (i.e., a nitrate supply mechanism). Note that these peak snowmelt nitrate concentrations (mean = 4.6 μeq/L [SE = 0.8]) are low relative to the historic record of volume weighted average monthly nitrate concentrations measured in W6 during the extended snowmelt period (March, April, and May), a time that is typically characterized by high nitrate pulses [*Bernhardt et al.*, 2005]. As predicted by *Schaefer et al.* [1990] for waters near 0 μeq/L ANC, episodic acidification at the HBEF appears to be under dual control (i.e., both C_B dilution and nitrate supply mechanisms). Base cation dilution remained important throughout the snowmelt period, as small decreases in C_B may represent a large proportion of the ANC in low-ANC waters. Nitrate supply was important only in the initial high-flow event of snowmelt, as the nitrate:sulfate equivalent ratio increased by an order of magnitude from base flow (~0.02 to 0.25, calculated from data in Table 2 [*Sullivan et al.*, 1997]). This short-term contribution of nitrate is consistent with the initial flushing

Table 3. Soil Solution Chemistry During Snowmelt in Subcatchments Along an Elevational Gradient in W6[a]

Site/Horizon	pH	ANC (μeq/L)	Al_m (μmol/L)	Al_i (μmol/L)	Al_o (μmol/L)	Al_i/Al_m	SO_4^{2-} (μmol/L)	NO_3^- (μmol/L)	DOC (μmol/L)	$[A^-]$ (μeq/L)	As (μeq/L)	Aw (μeq/L)	Aw/$[A^-]$	$[A^-]$/DOC ($(\mu eq/L)/(\mu mol/L)$)
Spruce-fir-birch														
Oa	4.20 (0.19)	−60.2 (35.2)	16.2 (0.20)	6.3 (0.3)	9.9 (0.2)	0.39	40.4 (3.3)	17.5 (14.8)	999.9 (79.8)	35.1 (2.0)	29.0 (6.9)	6.1 (4.9)	0.18 (0.15)	0.035 (0.001)
Bh	4.22 (0.06)	−54.3 (12.5)	20.4 (1.6)	9.5 (2.2)	10.9 (0.6)	0.47	47.1 (8.5)	33.2 (23.7)	888.6 (130.2)	7.9 (19.7)	9.5 (9.5)	4.3 (4.3)	0.16 (0.16)	0.006 (0.021)
Bs	4.65 (0.07)	−1.1 (7.1)	18.2 (2.1)	9.2 (3.4)	9.0 (1.3)	0.51	41.7 (0.6)	1.4 (1.2)	662.2 (157.4)	56.4 (37.1)	42.1 (38.6)	14.3 (1.5)	0.48 (0.34)	0.104 (0.081)
High hardwood														
Oa	4.46	−24.8	20.5	14.1	6.4	0.69	35.3	10.3	435.4	14.2	7.1	7.2	0.51	0.033
Bh	4.34	−38.9	14.9	6.3	8.6	0.42	24.7	2.2	737.0	27.2	22.1	5.1	0.19	0.037
Bs	4.79	−2.7	19.0	14.9	4.1	0.78	33.6	0.2	277.2	−0.9	-	-	-	−0.003
Low hardwood														
Oa	4.69 (0.07)	−12.8 (4.7)	10.9 (1.2)	7.1 (0.6)	3.8 (0.9)	0.65	33.8 (0.9)	6.7 (0.7)	288.2 (55.8)	9.8 (2.5)	4.6 (1.4)	5.2 (3.0)	0.42 (0.24)	0.033 (0.006)
Bh	4.85 (0.03)	−2.6 (1.4)	10.7 (0.1)	7.9 (0.2)	2.8 (0.04)	0.73	36.3 (2.3)	1.6 (0.2)	213.3 (11.2)	4.0 (0.1)	0.37 (0.37)	3.6 (0.2)	0.91 (0.10)	0.019 (0.002)
Bs	4.95 (0.06)	2.5 (2.3)	9.9 (1.4)	7.7 (1.4)	2.2 (0.1)	0.78	37.1 (2.8)	3.8 (1.3)	182.5 (4.4)	1.0 (4.2)	0	1.0 (4.2)	1.0	0.005 (0.024)

[a]W6 is the reference watershed at the HBEF. Samples were collected 28 April 2005. The spruce-fir-birch, high hardwood, and low hardwood subcatchments are represented by two, one, and three lysimeter pits, respectively, as complete data required to make organic acid anion calculations were missing from some lysimeter pits. Values in parentheses show 1 SE.

of mineralization by-products from soil during the early phase of snowmelt [*Sebestyen et al.*, 2008].

3.3.2. Aluminum Mobilization

[30] Aluminum usually fluctuates in concert with nitrate during snowmelt driven acid episodes; however, in this study, stream concentrations of aluminum remained elevated after nitrate concentrations declined (Table 2). Thus, aluminum made up most of the deficit in positive charge due to dilution of base cation concentrations throughout snowmelt (Figure 4). Although aluminum mobilization buffers against decreases in ANC [*Driscoll and Postek*, 1995], a large percentage of free acidity during snowmelt (29%–36%), and in base flow after snowmelt (43%), resulted from hydrolysis of mobile Al_i (the toxic form of aluminum).

[31] Aluminum is mobilized from the forest floor by both strong inorganic and strong organic acids [e.g., *David and Driscoll*, 1984; *McDowell and Wood*, 1984; *Driscoll et al.*, 1985; *Driscoll and Postek*, 1995]. Both Al_i and Al_m concentrations in soil solutions were equal to or greater than Al_i and Al_m concentrations in stream water (Tables 3 and 4). As DOC decreased vertically through the soil profile, with elevation down through subcatchments, and downstream during snowmelt, the proportion of Al_m as Al_i increased. At the weir, Al_i accounted for 44.6% of Al_m in preevent base flow, and nearly doubled to 74.6% (SE = 2.0%) throughout the snowmelt period. In contrast, in a high-DOC stream at the HBEF (W9, a north facing conifer-dominated watershed), increases in Al_m were mainly due to increases in Al_o [*Wellington and Driscoll*, 2004]. Nonetheless, our results generally agree with other studies of aluminum speciation during high-flow events showing that Al_i increases with decreases in pH [*Driscoll et al.*, 1980, 1984; *Driscoll and Postek*, 1995]. This pattern suggests that episodic aluminum mobilization in dilute systems may result in high concentrations of Al_i due to limitations of DOC to bind Al_i.

[32] Inorganic monomeric aluminum (Al_i) concentrations exceeded the ~2 μmol/L threshold known to be toxic to fish when flows were still low at the onset of snowmelt, and Al_i remained elevated throughout the snowmelt period regardless of flow conditions (2.5–7.3 μmol/L, Q = 3.1–93.4 L/s (Figure 4) [*Baker et al.*, 1996; *Van Sickle et al.*, 1996; *MacAvoy and Bulger*, 1995; Gagen et al.,1994; *Baker and Schofield*, 1982; *Driscoll et al.*, 1980]). Whereas decreases in volume weighted average monthly concentrations of Al_i [*Palmer and Driscoll*, 2002], sulfate [*Likens et al.*, 2002], nitrate [*Bernhardt et al.*, 2005], and calculated alkalinity (C_{ALK} (Figure 5)) exported from W6 during snowmelt over the historic record may be indicative of some recovery from soil acidification, observations of high stream Al_i and nitrate concentrations during snowmelt in this study somewhat contradict the notion of recovery from acidification.

3.3.3. Dissolved Organic Carbon, Organic Acid Anions, and Total Suspended Solids

[33] Dissolved organic carbon (DOC), and organic acid anion (A^-) concentrations in stream water increased during snowmelt, despite the typically dilute nature of this system. TSS was nearly undetectable, but concentrations increased during the highest flows (4.4 and 17.0 mg/L TSS, at 70.2 and 93.4 L/s discharge, respectively (Figure 6)). DOC concentrations ranged from 109.7 to 278.9 μmol C/L, and correlated strongly with discharge ($r^2 = 0.82$, $p < 0.0001$ (Figure 6)).

Table 4. Stream Chemistry Along an Elevational Gradient in W6[a]

Stream Site	pH	ANC (μeq/L)	Al_m (μmol/L)	Al_i (μmol/L)	Al_o (μmol/L)	Al_i/Al_m	SO_4^{2-} (μmol/L)	NO_3^- (μmol/L)	DOC (μmol/L)	$[A^-]$ (μeq/L)	As (μeq/L)	Aw (μeq/L)	$Aw/[A^-]$	$[A^-]$/DOC ((μeq/L)/(μmol/L))
1	4.15	−61.6	9.2	1.6	7.5	0.17	25.3	0.4	1356.4	64.2	56.3	7.9	0.1	0.047
2	4.32	−40.7	10.7	3.6	7.1	0.34	29.3	4.9	803.3	23.4	16.2	7.2	0.3	0.029
3	4.49	−24.5	12.5	7.0	5.5	0.56	33.0	7.0	474.7	12.4	5.0	7.4	0.6	0.026
4	4.64	−17.7	12.5	9.0	3.6	0.72	35.8	5.1	286.8	4.4	0	4.4	1.0	0.015
5	4.74	−13.2	10.5	7.5	2.9	0.71	35.9	3.8	244.7	3.9	0	3.9	1.0	0.016
7	4.95	−5.4	7.7	5.5	2.2	0.71	37.4	2.2	197.5	−2.1	-	-	-	−0.01

[a]W6 is the reference watershed at the HBEF. Samples were collected 28 April 2005. Stream site locations are shown in Figure 1.

Not surprisingly, organic acid anion (A^-) concentrations increased with increases in DOC ($r^2 = 0.78$, $p < 0.0001$ (Figure 4)). With respect to acidification processes, organic acid anions were assumed to provide the balancing negative charge [*Driscoll et al.*, 1989, 1994]; this was reflected by the greater concentration of (A^-) released in the final high-flow event (24 April, DOY 115) as the initial flushing of nitrate subsided and Al_i concentrations remained elevated. This pattern may suggest that aluminum was mobilized from within shallow soils by strong organic acids (especially late in snowmelt) in addition to being mobilized by strong inorganic acids (i.e., nitrate) which was more evident during early snowmelt.

[34] All organic acids in stream water draining W6 during snowmelt were weakly acidic (as calculated with equations (7)–(9)), a result somewhat inconsistent with research on the nature of organic acids in the northeastern United States. For example, *Wellington and Driscoll* [2004] found that most organic acids in W9 stream water were strongly acidic in nature (W9 is a north facing conifer-dominated watershed). In an Adirondack lake survey, *Driscoll et al.* [1994] found about one third of organic acids to be strongly acidic. *Munson and Gherini* [1993] showed that organic acids contain a range of acidic functional groups (many of which display weak acid characteristics) with a substantial fraction as strong acids (i.e., $pK_a < 3$). *Kramer et al.* [1990] showed that organic acids at high-elevation lakes (>530 m) in the USEPA's Eastern Lakes Study had a predominance of organic acids with low pK_a values, shifting to higher pK_a values (i.e., weaker organic acids) at lower elevations. *Kramer et al.* [1990] suggest that this shift results, in part, from degradation of low pK_a low molecular weight organic acids, and the production of stable phenolic compounds at lower elevations associated with increasing hydrologic residence times. *Kramer et al.* [1990] further suggest that the elevation and residence time patterns of DOC degradation result from differences in flow paths through the watershed. The hypothesis of *Kramer et al.* [1990] is consistent with observations of organic acids along vertical gradients within the soil profile and along longitudinal stream gradients at Hubbard Brook (note W6 weir elevation at ~540 m). Specifically, the proportion of weak acids (i.e., $[A_w]/[A^-]$) generally increased with increasing soil depth (Table 3) and along the longitudinal gradient within the stream (Table 4). Thus, organic acids in solutions sampled from shorter more shallow hydrologic flow paths were less processed and more strongly acidic in nature than organic acids in solutions sampled from longer flow paths. Ultimately, the prevalence of weak acids in stream water at the weir suggests that DOC associated with shallow flow paths and strong organic acid anions at the top of the watershed is either diluted or rapidly processed, or both, before being delivered to the weir, even during the snowmelt period.

[35] The charge density of organic acid anions ($[A^-]$/[DOC], μeq/μmol) increased from −0.025 to 0.050 μeq/μmol mol (pH 4.8–5.3) across the hydrograph in conjunction with higher flows and greater concentrations of DOC. This pattern was likely due to changes in the character of stream DOC from different soil horizons and/or source areas of the watershed that became more hydrologically connected to the stream under high-flow conditions [*Dittman et al.*, 2007; *Lawrence and Driscoll*, 1990; *Hooper and Shoemaker*, 1986] (see section 3.2).

3.3.4. Multiple Mechanisms of Episodic Acidification

[36] Multiple mechanisms influence episodic acidification across the snowmelt hydrograph in the dilute waters of the reference watershed at the HBEF. Dilution of base cations is important throughout the snowmelt period. Nitrate and aluminum acidity drove ANC to negative values only during the initial high-flow event of snowmelt, whereas aluminum acidity persisted throughout the snowmelt event, even after nitrate concentrations declined. Finally, low concentrations of DOC and associated organic acids appeared to play a key role in acidification processes throughout snowmelt, with the role of [A−] persisting and becoming proportionally more important after nitrate concentrations declined later in the event. These results mostly agree with the results from the Episodic Response Project [*Wigington et al.*, 1996], which concluded that base cation dilution and organic acid production were the most important ion changes during episodic acidification (as based on absolute changes), with nitrate more important in snowmelt driven events and organic acids more important in coniferous and mixed deciduous forests. Thus, given that W6 at the HBEF is a mixed coniferous and deciduous forest with a substantial snowpack, and that stream water ANC is typically near 0 μeq/L, the three mechanisms hypothesized to be important based on these watershed characteristics all did influence acidification during snowmelt. Ultimately, differences in hydrologic source areas and flow paths within (and among) watersheds are key drivers of differences in mechanisms resulting in episodic acidification.

3.4. Episodic Mercury Mobilization

[37] Shifts in hydrologic source areas and flow paths that influence the source and character of the DOC supply to streams not only drives episodic acidification and aluminum mobilization, but also influences the transport of mercury from terrestrial soils to aquatic ecosystems.

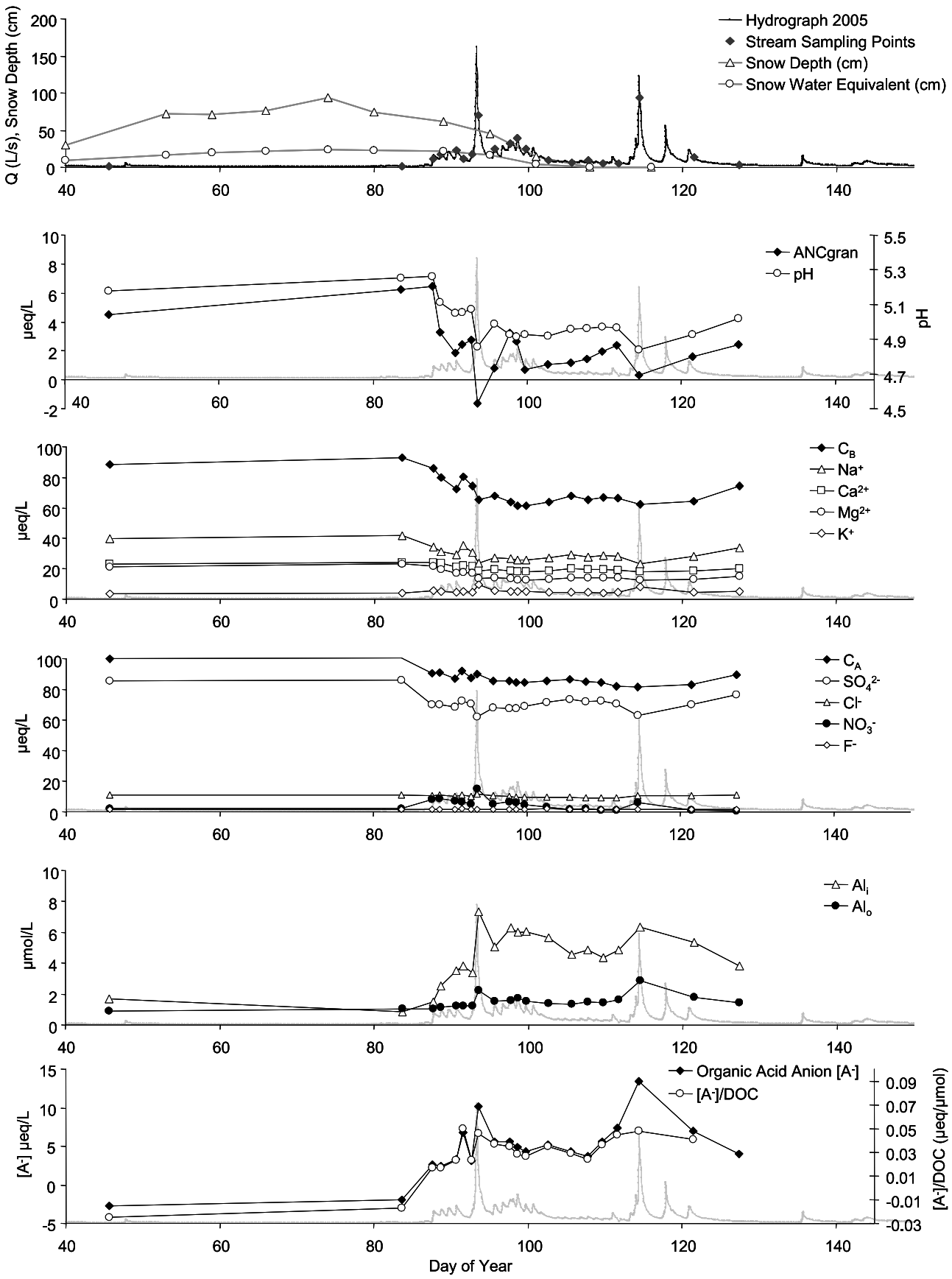

Figure 4. Snowpack, discharge, and stream concentrations of major solutes that regulate the acid-base status of W6 during snowmelt at the Hubbard Brook Experimental Forest.

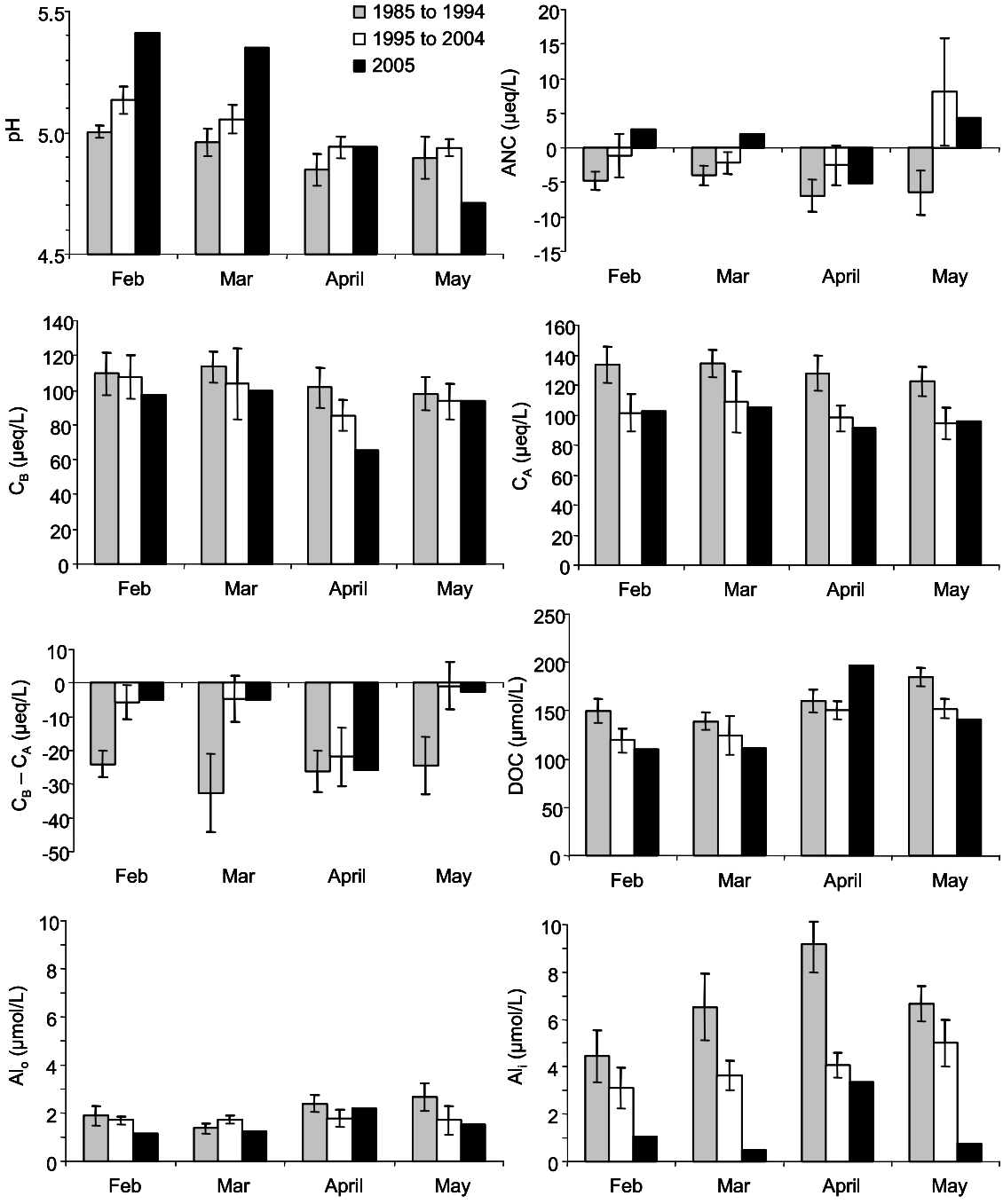

Figure 5. Historic record of stream water chemistry during snowmelt months at the weir in W6, the reference watershed at the HBEF. Data are average concentrations from monthly sampling. Error bars indicate +/− 1 SE (C. T. Driscoll, unpublished data, 1984–2005).

3.4.1. Mercury Concentration and Flux

[38] Mercury concentrations observed in W6 stream water at the HBEF, even during high-flow events, are low compared to concentrations of mercury in stream water from other watershed studies [*Shanley et al.*, 2002; *Babiarz et al.*, 1998; *Hurley et al.*, 1998; *Scherbatskoy et al.*, 1998; *Bishop et al.*, 1995; *Krabbenhoft et al.*, 1995]. The low mercury concentrations are not surprising, as W6 has limited wetlands, few seeps, is dominated by upland deciduous forest (~85%), and exhibits low concentrations of TSS and DOC. Annual wet deposition of mercury at the HBEF is ~8.7 $\mu g/m^2$ yr (MDN site NH02, available data spanned February 2004 through February 2005). Hydrologic connectivity between surficial terrestrial soils and the aquatic ecosystem is more spatially and temporally limited in this watershed than in watersheds with a greater percent area of wetlands, thus restricting transfer of dissolved mercury from forests to streams. Moreover, deciduous forests likely deposit less mercury to the forest floor than do conifer forests and deliver more of that mercury with leaf litter rather than in

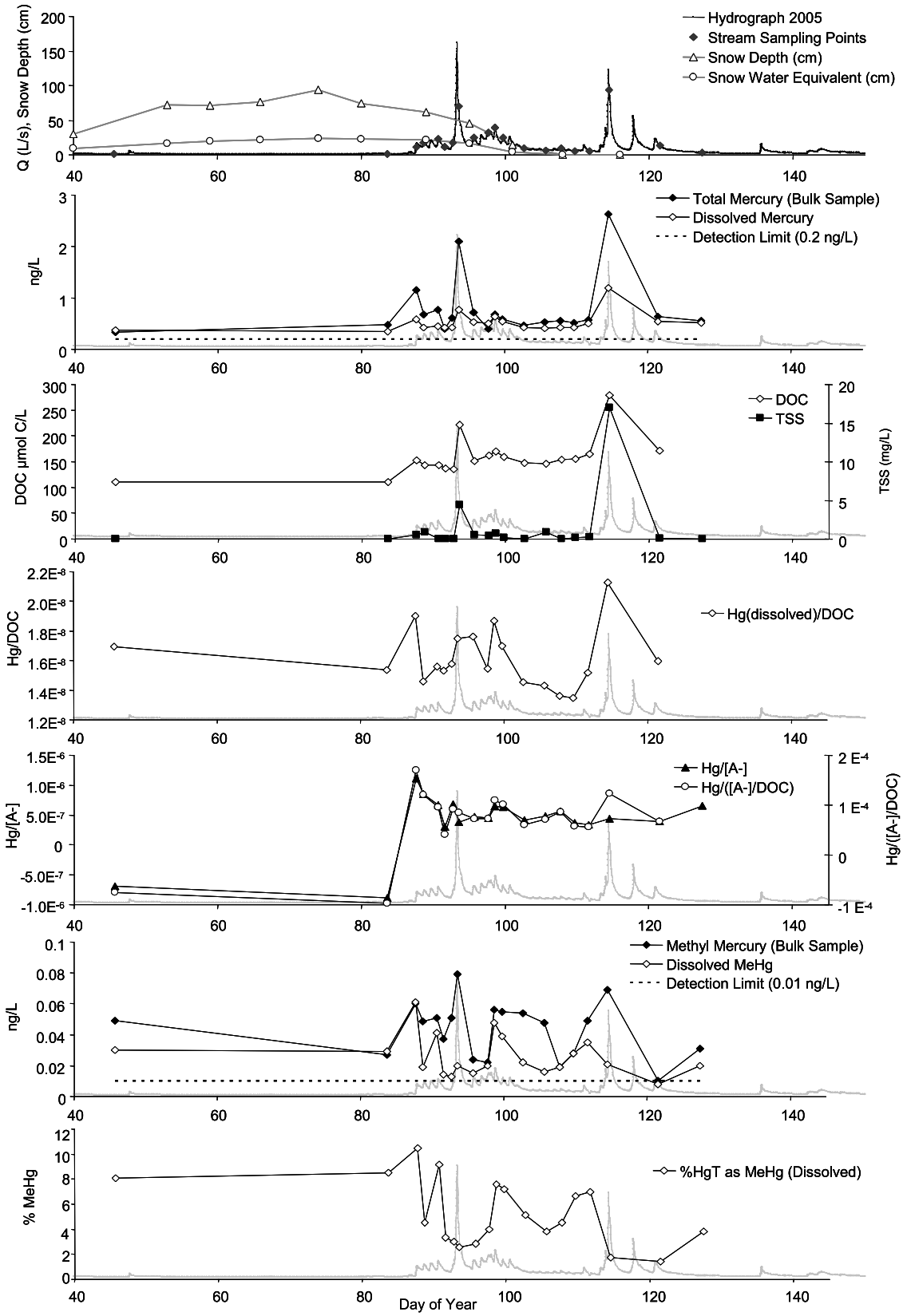

Figure 6. Snowpack, discharge, and stream concentrations of mercury species, DOC, and organic acid anions during snowmelt at W6 at the Hubbard Brook Experimental Forest.

throughfall, which may affect the ultimate fate of mercury in the ecosystem [*Demers et al.*, 2007]. Thus, W6 at the HBEF is an end-member watershed representing an ecosystem that should export limited mercury to streams and down-gradient aquatic ecosystems.

[39] Average preevent base flow stream concentrations of mercury were 0.41 ng/L for bulk samples and 0.36 ng/L for the dissolved fraction (<0.45 μm (Figure 6)). Stream water concentrations of bulk total mercury (Hg_t) increased exponentially with flow ($R^2 = 0.69$, $p < 0.0001$), reaching 2.6 ng/L at an instantaneous flow of 93.4 L/s; concentrations of dissolved mercury (Hg_d) also increased exponentially with flow to a maximum concentration of 1.2 ng/L ($R^2 = 0.83$, $p < 0.0001$ (PROC REG (SAS Institute Inc., SAS OnlineDoc, version 8, Cary, North Carolina, 1999, hereafter SAS Institute Inc., 1999))) (Figure 6). These patterns contrast with snowmelt at Sleepers River Vermont where *Shanley et al.* [2002] measured order of magnitude higher particulate mercury (Hg_p) concentrations (16 ng/L) and two times higher dissolved mercury concentrations (2 ng/L) compared to W6 at the HBEF. High-flow conditions result in a range of responses in mercury export from wetland and forest ecosystems.

[40] The exponential relationship between mercury concentration and discharge implies that a disproportionate amount of mercury export occurs during high-flow events. The total amount of mercury exported from W6 during the snowmelt period (24 March to 7 May 2005) was 59.8 mg. Estimated mercury fluxes from the two largest snowmelt peaks were 24.2 mg (DOY 92.3–95.4) and 13.3 mg (DOY 113.6–117.2), respectively. Thus, nearly two thirds (63%) of the mercury export from the entire snowmelt period occurred during two high discharge events that represented only a third of total discharge and 15% of total duration of the snowmelt. For illustrative purposes, we estimated total annual export of mercury from W6 using the concentration: flow relationship developed for the snowmelt period coupled to the annual hydrograph. Based on this estimate, the snowmelt period accounted for 35% of estimated total annual mercury export (172.7 mg); the five peak flows of the annual hydrograph that exceeded 100 L/s (which include two peak snowmelt flows) accounted for 72% of estimated annual export of total mercury and 78% of estimated annual export of dissolved mercury.

[41] Transport of mercury associated with both the dissolved and particulate fractions substantially contributed to mercury export during snowmelt. However, the dissolved fraction was more important during high flows at the HBEF than observed in Vermont for high-flow events in forested ecosystems [e.g., *Shanley et al.*, 2002; *Scherbatskoy et al.*, 1998], with the particulate fraction dominating only at the highest flows (Figure 6). Across the entire snowmelt hydrograph, the percentage of Hg_t concentration accounted for by the dissolved fraction ranged from 37% to 100% of Hg_t concentrations (mean 77.5%, SE 5.8, n = 20). Dissolved mercury (Hg_d) accounted for 37% and 46% of Hg_t flux during the two highest snowmelt peaks, and was 53% of the total mercury flux during the entire snowmelt period. These fractions of Hg_d were large in comparison to the partitioning of mercury at peak snowmelt in Vermont (only 12.5% Hg_d, as calculated from data by *Shanley et al.* [2002]). Moreover, mercury transported in the dissolved phase may be more bioavailable for methylation in downstream aquatic ecosystems than mercury associated with particulate matter [*Munthe et al.*, 2007]. Thus, both the particulate and dissolved phases of mercury are important contributions to Hg_t export during snowmelt at the HBEF.

3.4.2. Methyl Mercury Concentration and Flux

[42] In contrast with Hg_t, discharge explained only a moderate amount of the variability in particulate associated MeHg ($MeHg_p$; $r^2 = 0.34$, $p = 0.008$), and was not related to the variation in dissolved MeHg ($MeHg_d$) ($p = 0.81$ (PROC REG (SAS Institute Inc., 1999))). Methyl mercury concentrations ranged from 0.01 to 0.08 ng/L in bulk samples (mean 0.04 ng/L, SE 0.007 ng/L, n = 20) and from <0.01 to 0.06 ng/L in the dissolved phase (mean 0.03 ng/L, SE 0.002 ng/L, n = 20); $MeHg_d$ accounted for 25%–100% of the MeHg in bulk samples (Figure 6). The percentage of Hg_t as MeHg was large, ranging from 1.6% to 14.5% in bulk samples and from 1.4% to 10.4% in filtered samples. Note that the %MeHg values are based on small MeHg and Hg_t values, and should be interpreted with caution. Nonetheless, the percentage of Hg_d as MeHg (i.e., %MeHg) across the hydrograph revealed an intriguing pattern; the %MeHg peaked just after the first small snowmelt peak on the hydrograph (10.4% MeHg; 10.9 L/s (Figure 6)). Proceeding from this first flush, and as discharge continued to increase, the %MeHg declined (Figure 6). Subsequent peaks in %MeHg tended to occur on rising limbs of the hydrograph, possibly as different hydrologic source areas in the watershed began to contribute shallow soil water to stream flow. This pattern may suggest that MeHg is produced within forest soils under winter conditions and that MeHg pools in soil solutions are diluted as flushing exceeds production. Alternate explanations for the observed patterns are possible (e.g., demethylation dynamics, or a spike in methylation at snowmelt); however, it is difficult to evaluate the mechanism responsible for these patterns without mercury data from within the forest soil pools.

3.4.3. Mercury, TSS, DOC, and Organic Acid Anion Charge Density

[43] Despite relatively low concentrations, DOC and TSS appear to influence mercury dynamics at the HBEF. Dissolved mercury (Hg_d) was more strongly correlated with DOC ($r^2 = 0.91$, $p < 0.0001$) than particulate mercury (Hg_p) was with TSS ($r^2 = 0.40$, $p < 0.01$ (PROC REG (SAS Institute Inc., 1999))). As mercury has been shown to correlate with organic carbon [e.g., *Meili*, 1991], it is not surprising that peaks in Hg_p and Hg_d coincided with peaks in TSS and DOC, respectively (Figure 6). However, the quantity of mercury transported by DOC on a per mol basis (Hg_d/DOC) varied by more than 50% over the hydrograph (1.3×10^{-8} to 2.1×10^{-8}), and the ratio of Hg_d to organic acid anion charge density ($Hg_d/([A^-]/DOC)$) followed a similar pattern, varying by more than 300% across the hydrograph (Figure 6). Thus, increases in mercury transport may not simply be due to increases in DOC concentration alone, but may also be influenced by the source and associated character of the DOC.

[44] Statistical models that distinguish between hydrologic source areas within the watershed help explain fluctuations in (Hg_d/DOC), [$Hg_d/([A^-]/DOC)$], and Hg_d. Mercury transported per unit DOC on a per mol basis (Hg_d/DOC) was correlated with total discharge alone ($r^2 = 0.50$, $p < 0.001$);

however, when the discharge originating from specific hydrologic source areas was considered, the amount of discharge from shallow soils of the HH/SFB explained as much of the variation in (Hg_d/DOC) as did total discharge ($r^2 = 0.50$, $p < 0.001$ (PROC REG (SAS Institute Inc., 1999))). Also, mercury per unit charge density [Hg_d/([A^-]/DOC)] was not well correlated with total discharge alone ($r^2 = 0.17$, $p = 0.08$); whereas, a statistical model including total discharge and the percentage of total discharge originating from shallow soils in the LH and HH/SFB explained much more of the variation in Hg_d/([A^-]/DOC) ($r^2 = 0.86$, $p < 0.0001$ (PROC REG (SAS Institute Inc., 1999))). Moreover, stream water Hg_d was also better explained by a model that distinguished between hydrologic source areas within the watershed; that is, all of the variability in the spatially explicit model could be explained by the amount of discharge originating from shallow soils in the HH/SFB zone ($r^2 = 0.92$, $p < 0.0001$ (PROC REG (SAS Institute Inc., 1999))). Thus, these discrete shifts in mercury density on DOC suggest the influence of DOC that varies both in character and contributing source area within the watershed.

[45] Observed changes in the character of DOC corroborate changes in the hydrologic flow paths predicted by our hydrograph separation model. Soil solutions within the hardwood subcatchments show greater DOC concentrations, greater [A^-], and greater ([A−]/DOC) in more shallow soils (i.e., Oa and Bh horizons) than in lower mineral horizons (i.e., Bs horizon (Table 3)). Soil solutions within the SFB subcatchment lack a distinct pattern along the soil depth profile; however, shallow soil solutions in the HH and SFB zone have greater DOC and [A^-] concentrations than soil solutions in corresponding horizons in the LH zone (Table 3). Along an elevational gradient within the stream, DOC concentrations, [A^-], and ([A^-]/DOC) are greatest in the SFB zone at the top of the watershed, and decrease downstream (Table 4). This elevational pattern within the stream may, in part, be due to dilution effects or in-stream abiotic sorption of DOC, or both [*McDowell*, 1985]. Whereas *McDowell* [1985] found biotic processing of DOC to be minimal in the stream draining W6, recent work in other regions suggest that DOC character may be microbially altered within the stream ecosystem [e.g., *Frost et al.*, 2006; *Young et al.*, 2004]. Nevertheless, changes in DOC character across the hydrograph coincide with shifts in source areas and flow paths modeled by our hydrograph separation. Hydrologically induced changes in DOC character also have been demonstrated in other studies. In a small watershed associated with a fen wetland, *Maurice et al.* [2002] found that the contribution of soil pore water relative to groundwater influenced both the concentration and character of natural organic matter in streams. In the Colorado Rockies, *Hood et al.* [2005] showed that seasonal shifts in the chemical character of DOM resulted from changes in the source of that DOM. *Dai et al.* [2001] studied organic matter chemistry at the HBEF and concluded that variation in hydrologic flow paths are important in regulating the organic matter chemistry of stream water. Hence, increased mercury transport during high-flow events is not simply due to an increase in the concentration of the same DOC that is exported at base flow, but instead there appears to be a shift in the source area and associated character of DOC (as inferred above from Hg:DOC ratios). *Shanley et al.* [2008] showed that the Hg:DOC ratio in stream water increased as snowmelt progressed at Sleepers River in Vermont and suggested that Hg was associated with a particular fraction of DOC. Clearly, the character and contributing source of DOC influences the transport of dissolved mercury at the HBEF and likely in other forested watersheds. Ultimately, differences in hydrology within (and among) watersheds determines contributing source areas and hydrologic flow paths that influence the concentration and character of DOC (and POC) which, in turn, drives concentrations and fluxes of dissolved (and particulate) mercury transported from terrestrial to aquatic ecosystems.

4. Conclusions and Implications

[46] DOC plays a key role in episodic acidification and mercury transport during snowmelt at the HBEF, even though DOC concentrations are relatively low. The supply of DOC that links episodic acidification by natural organic acids and mobilization of dissolved mercury is governed by shifts in hydrologic flow paths and contributing source areas. This research highlights the importance of spatially and temporally dynamic hydrologic connectivity between the uplands and the aquatic ecosystem, and this dynamic hydrologic connectivity influences how we should (1) assess stream solute loads given the discharge-dependent chemistry and (2) consider the environmental consequences of the timing and distribution of the delivery of those loads to surface waters (e.g., pulses of toxic concentrations of labile (inorganic) monomeric aluminum and elevated loads of total mercury). Ultimately, terrestrial ecosystems mediate the transfer of atmospheric deposition from uplands to aquatic ecosystems, imposing lags upon the recovery of surface waters despite decreases in atmospheric emissions and deposition of pollutants.

[47] Note that for this end-member site representing (1) limited recovery from acidification; (2) low concentrations of dissolved organic carbon; and (3) low mercury deposition and export, small increases in DOC export associated with high flows are linked to mercury export from terrestrial ecosystems to surface waters. Thus, processes that generate and mobilize DOC within the watershed ultimately control mercury export dynamics from terrestrial ecosystems.

[48] Recently, some watersheds in North America and Europe have begun to recover from chronic acid deposition [*Stoddard et al.*, 1999; *Skjelkvale et al.*, 2001; *Driscoll et al.*, 2003]. However, the degree of recovery of surface water pH and ANC has been less than expected with respect to measured declines in sulfate emissions and deposition, buffered in part by concomitant increases in DOC [*Stoddard et al.*, 2003; *Driscoll et al.*, 2003; *Skjelkvale et al.*, 2001, 2005]. It is possible that there also has been a concomitant increase in mercury export from terrestrial ecosystems (i.e., based on DOC-Hg relationships), and this may be one possible mechanism explaining the long-term decrease in mercury retention within the terrestrial ecosystem [*Lorey and Driscoll*, 1999; *Engstrom and Swain*, 1997] (see section 1). Increases in DOC export that might bind and therefore detoxify Al_i may, at the same time, exacerbate mercury mobilization. As ecosystems continue to recover from chronic acidification and respond to broader environmental change, shifting DOC dynamics will likely play an important role in the transfer of both aluminum and mercury loads from uplands to surface waters.

[49] **Acknowledgments.** We thank Janet Towse for assistance in the field and Mario Montesdeoca for technical laboratory support. The USDA Forest Service has provided hydrologic and climatic data, and their support has been invaluable to this study. This research was supported with funding from the Small Grants Program within the NSF IGERT Program in Biogeochemistry and Environmental Biocomplexity at Cornell University and the NSF Long-Term Ecological Research (46222-7759) program at Hubbard Brook. Some data used in this publication were obtained by scientists of the Hubbard Brook Ecosystem Study; this publication has not been reviewed by those scientists. The Hubbard Brook Experimental Forest is operated and maintained by the Northern Research Station, U.S. Department of Agriculture, Newton Square, Pennsylvania.

References

Babiarz, C. L., J. P. Hurley, J. M. Benoit, M. M. Shafer, A. W. Andren, and D. A. Webb (1998), Seasonal influences on partitioning and transport of total and methylmercury in rivers from contrasting watersheds, *Biogeochemistry*, *41*, 237–257, doi:10.1023/A:1005940630948.

Bailey, A. S., J. W. Hornbeck, J. L. Campbell, and C. Eager (2003), Hydrometeorological database for Hubbard Brook Experimental Forest: 1955–2000, *Gen. Tech. Rep. NE-305*, 36 pp., Northeast. Res. Stn., U.S. Dep. of Agric. For. Serv., Newton Square, Pa.

Baker, J. P., and C. L. Schofield (1982), Aluminum toxicity to fish in acidic waters, *Water Air Soil Pollut.*, *18*, 289–309, doi:10.1007/BF02419419.

Baker, J. P., et al. (1996), Episodic acidification of small streams in the northeastern United States: Effects on fish populations, *Ecol. Appl.*, *6*, 422–437, doi:10.2307/2269380.

Balogh, S. J., E. B. Swain, and Y. H. Nollet (2006), Elevated methylmercury concentrations and loadings during flooding in Minnesota rivers, *Sci. Total Environ.*, *368*, 138–148, doi:10.1016/j.scitotenv.2005.09.045.

Bernhardt, E. S., et al. (2005), Can't see the forest for the stream?: In-stream processing and terrestrial nitrogen exports, *BioScience*, *55*, 219–230, doi:10.1641/0006-3568(2005)055[0219:ACSTFF]2.0.CO;2.

Bishop, K., Y.-H. Lee, C. Pettersson, and B. Allard (1995), Methylmercury output from the Svartberget Catchment in northern Sweden during spring flood, *Water Air Soil Pollut.*, *80*, 445–454, doi:10.1007/BF01189694.

Branfireun, B. A., D. Hilbert, and N. T. Roulet (1998), Sinks and sources of methylmercury in a boreal catchment, *Biogeochemistry*, *41*, 277–291, doi:10.1023/A:1005964603828.

Burns, D. A., J. J. McDonnell, R. P. Hooper, N. E. Peters, J. E. Freer, C. Kendall, and K. Beven (2001), Quantifying contributions to storm runoff through end-member mixing analysis and hydrologic measurements at the Panola Mountain Research Watershed (Georgia, USA), *Hydrol. Process.*, *15*, 1903–1924, doi:10.1002/hyp.246.

Campbell, J. L., M. J. Mitchell, and B. Mayer (2006), Isotopic assessment of NO_3^- and SO_4^{2-} mobility during winter in two adjacent watersheds in the Adirondack Mountains, New York, *J. Geophys. Res.*, *111*, G04007, doi:10.1029/2006JG000208.

Chen, C. W., S. A. Gherini, N. E. Peters, P. S. Murdoch, R. M. Newton, and R. A. Goldstein (1984), Hydrologic analyses of acidic and alkaline lakes, *Water Resour. Res.*, *20*, 1875–1882, doi:10.1029/WR020i012p01875.

Christophersen, N., and R. P. Hooper (1992), Multivariate analysis of stream water chemical data: The use of principal components analysis for the end-member mixing problem, *Water Resour. Res.*, *28*, 99–107, doi:10.1029/91WR02518.

Cirmo, C. P., and C. T. Driscoll (1993), Beaver pond biogeochemistry: Acid neutralizing capacity generation in a headwater wetland, *Wetlands*, *13*, 277–292.

Dahlgren, R. A., and C. T. Driscoll (1994), The effects of whole-tree clear-cutting on soil processes at the Hubbard Brook Experimental Forest, New Hampshire, USA, *Plant Soil*, *158*, 239–262, doi:10.1007/BF00009499.

Dai, K. H., C. E. Johnson, and C. T. Driscoll (2001), Organic matter chemistry and dynamics in clear-cut and unmanaged hardwood forest ecosystems, *Biogeochemistry*, *54*, 51–83, doi:10.1023/A:1010697518227.

David, M. B., and C. T. Driscoll (1984), Aluminum speciation and equilibria in soil solutions of a Haplorthod in the Adirondack Mountains (New York, U.S.A.), *Geoderma*, *33*, 297–318, doi:10.1016/0016-7061(84)90031-4.

De Coninck, F. (1980), Major mechanisms in formation of spodic horizons, *Geoderma*, *24*, 101–128, doi:10.1016/0016-7061(80)90038-5.

Demers, J. D., C. T. Driscoll, J. B. Yavitt, and T. J. Fahey (2007), Mercury cycling in litter and soil in different forest types in the Adirondack region, New York, USA, *Ecol. Appl.*, *17*, 1341–1351, doi:10.1890/06-1697.1.

Detty, J. M. (2008), Patterns and processes of two states: Watershed runoff as determined by a total soil water threshold, M.S. thesis, Plymouth State Univ., Plymouth, N. H.

Dittman, J. A., C. T. Driscoll, P. M. Groffman, and T. J. Fahey (2007), Dynamics of nitrogen and dissolved organic carbon at the Hubbard Brook Experimental Forest, *Ecology*, *88*, 1153–1166, doi:10.1890/06-0834.

Drexel, R. T., M. Haitzer, J. N. Ryan, G. R. Aiken, and K. L. Nagy (2002), Mercury (II) sorption to two Florida Everglades peats: Evidence for strong and weak binding and competition by dissolved organic matter released from the peat, *Environ. Sci. Technol.*, *36*, 4058–4064, doi:10.1021/es0114005.

Driscoll, C. T., and R. M. Newton (1985), Chemical characteristics of Adirondack lakes, *Environ. Sci. Technol.*, *19*, 1018–1024, doi:10.1021/es00141a604.

Driscoll, C. T., and K. M. Postek (1995), The chemistry of aluminum in surface waters, in *The Environmental Chemistry of Aluminum*, edited by G. Sposito, pp. 363–418, Lewis, New York.

Driscoll, C. T., and G. C. Schafran (1984), Short-term changes in the base neutralizing capacity of an acid Adirondack lake, New York, *Nature*, *310*, 308–310, doi:10.1038/310308a0.

Driscoll, C. T., J. P. Baker, J. J. Bisogni, and C. L. Schofield (1980), Effect of aluminum speciation on fish in dilute acidified waters, *Nature*, *284*, 161–164, doi:10.1038/284161a0.

Driscoll, C. T., J. P. Baker, J. J. Bisogni, and C. L. Schofield (1984), Aluminum speciation and equilibria in dilute acidified surface waters of the Adirondack region of New York State, in *Geological Aspects of Acid Deposition*, edited by O. P. Bricker, pp. 55–75, Butterworth, Boston, Mass.

Driscoll, C. T., N. vanBreemen, and J. Mulder (1985), Aluminum chemistry in a forested Spodosol, *Soil Sci. Soc. Am. J.*, *49*, 437–444.

Driscoll, C. T., C. P. Yatsko, and F. J. Unangst (1987), Longitudinal and temporal trends in the water chemistry of the north branch of the Moose River, *Biogeochemistry*, *3*, 37–61, doi:10.1007/BF02185184.

Driscoll, C. T., R. D. Fuller, and D. M. Simone (1988), Longitudinal variations in trace metal concentrations in a northern hardwood forested ecosystem, *J. Environ. Qual.*, *17*, 101–107.

Driscoll, C. T., R. D. Fuller, and W. D. Schecher (1989), The role of organic acids in the acidification of surface waters in the eastern U.S., *Water Air Soil Pollut.*, *43*, 21–40, doi:10.1007/BF00175580.

Driscoll, C. T., M. D. Lehtinen, and T. J. Sullivan (1994), Modeling the acid-base chemistry of organic solutes in Adirondack, New York, lakes, *Water Resour. Res.*, *30*, 297–306, doi:10.1029/93WR02888.

Driscoll, C. T., V. Blette, C. Yan, C. L. Schofield, R. Munson, and J. Holsapple (1995), The role of dissolved organic carbon in the chemistry and bioavailability of mercury in remote Adirondack lakes, *Water Air Soil Pollut.*, *80*, 499–508, doi:10.1007/BF01189700.

Driscoll, C. T., G. B. Lawrence, A. J. Bulger, T. J. Butler, C. S. Cronan, C. Eagar, K. F. Lambert, G. E. Likens, J. L. Stoddard, and K. C. Weathers (2001), Acidic deposition in the northeastern United States: Sources and inputs, ecosystem effects, and management strategies, *BioScience*, *51*, 180–198, doi:10.1641/0006-3568(2001)051[0180:ADITNU]2.0.CO;2.

Driscoll, C. T., K. M. Driscoll, K. M. Roy, and M. J. Mitchell (2003), Chemical response of lakes in the Adirondack region of New York to declines in acidic deposition, *Environ. Sci. Technol.*, *37*, 2036–2042, doi:10.1021/es020924h.

Engstrom, D. R., and E. B. Swain (1997), Recent declines in atmospheric mercury deposition in the upper Midwest, *Environ. Sci. Technol.*, *31*, 960–967, doi:10.1021/es9600892.

Frost, P. C., J. H. Larson, C. A. Johnston, K. C. Young, P. A. Maurice, G. A. Lamberti, and S. D. Bridgham (2006), Landscape predictors of stream dissolved organic matter concentration and physicochemistry in a Lake Superior river watershed, *Aquat. Sci.*, *68*, 40–51.

Gagen, C. J., W. E. Sharpe, and R. F. Carline (1993), Mortality of brook trout, mottled sculpins, and slimy sculpins during acidic episodes, *Trans. Am. Fish. Soc.*, *122*, 616–628.

Gagen, C. J., W. E. Sharpe, and R. F. Carline (1994), Downstream movement and mortality of brook trout (*Salvelinus fontinalis*) exposed to acidic episodes in streams, *Can. J. Fish. Aquat. Sci.*, *51*, 1620–1628, doi:10.1139/f94-162.

Grigal, D. F. (2002), Inputs and outputs of mercury from terrestrial watersheds: A review, *Environ. Rev.*, *10*, 1–39, doi:10.1139/a01-013.

Grigal, D. F. (2003), Mercury sequestration in forests and peatlands: A review, *J. Environ. Qual.*, *32*, 393–405.

Hood, E., M. W. Williams, and D. M. Mcknight (2005), Sources of dissolved organic matter (DOM) in a Rocky Mountain stream using chemical fractionation and stable isotopes, *Biogeochemistry*, *74*, 231–255, doi:10.1007/s10533-004-4322-5.

Hooper, R. P., and C. A. Shoemaker (1986), A comparison of chemical and isotopic hydrograph separation, *Water Resour. Res.*, *22*, 1444–1454, doi:10.1029/WR022i010p01444.

Hurley, J. P., J. M. Benoit, C. L. Babiarz, M. M. Shafer, A. W. Andren, J. R. Sullivan, R. Hammond, and D. A. Webb (1995), Influences of watershed characteristics on mercury levels in Wisconsin rivers, *Environ. Sci. Technol.*, *29*, 1867–1875, doi:10.1021/es00007a026.

Hurley, J. P., S. E. Cowell, M. M. Shafer, and P. E. Hughes (1998), Tributary loading of mercury to Lake Michigan: Importance of seasonal events and phase partitioning, *Sci. Total Environ.*, *213*, 129–137, doi:10.1016/S0048-9697(98)00084-9.

Johnson, C. E., C. T. Driscoll, T. G. Siccama, and G. E. Likens (2000), Element fluxes and landscape position in a northern hardwood forest watershed ecosystem, *Ecosystems*, *3*, 159–184, doi:10.1007/s100210000017.

Johnson, N. M., C. T. Driscoll, J. S. Eaton, G. E. Likens, and W. H. McDowell (1981), Acid-rain, dissolved aluminum and chemical-weathering at the Hubbard Brook Experimental Forest, New Hampshire, *Geochim. Cosmochim. Acta*, *45*, 1421–1437, doi:10.1016/0016-7037(81)90276-3.

Kamman, N. C., and D. R. Engstrom (2002), Historical and present fluxes of mercury to Vermont and New Hampshire lakes inferred from ^{210}Pb dated sediment cores, *Atmos. Environ.*, *36*, 1599–1609, doi:10.1016/S1352-2310(02)00091-2.

Khwaja, A. R., P. R. Bloom, and P. L. Brezonik (2006), Binding constants of divalent mercury (Hg^{2+}) in soil humic acids and soil organic matter, *Environ. Sci. Technol.*, *40*, 844–849, doi:10.1021/es051085c.

Kolka, R. K., D. F. Grigal, E. A. Nater, and E. S. Verry (2001), Hydrologic cycling of mercury and organic carbon in a forested upland-bog watershed, *Soil Sci. Soc. Am. J.*, *65*, 897–905.

Krabbenhoft, D. P., J. M. Benoit, C. L. Babiarz, J. P. Hurley, and A. W. Andren (1995), Mercury cycling in the Allequash Creek watershed, northern Wisconsin, *Water Air Soil Pollut.*, *80*, 425–433, doi:10.1007/BF01189692.

Kramer, J. R., P. Broussard, P. Collins, T. A. Clair, and P. Takats (1990), Variability of organic acids in watersheds, in *Organic Acids in Aquatic Ecosystems*, edited by E. M. Purdue and E. T. Gjessing, pp. 127–139, John Wiley, New York.

Lawrence, G. B., and C. T. Driscoll (1990), Longitudinal patterns of concentration discharge relationships in stream water draining the Hubbard Brook Experimental Forest, New Hampshire, *J. Hydrol.*, *116*, 147–165, doi:10.1016/0022-1694(90)90120-M.

Likens, G. E., and F. H. Bormann (1995), *Biogeochemistry of a Forested Ecosystem*, 2nd ed., Springer, New York.

Likens, G. E., C. T. Driscoll, D. C. Buso, M. J. Mitchell, G. M. Lovett, S. W. Bailey, T. G. Siccama, W. A. Reiners, and C. Alewell (2002), The biogeochemistry of sulfur at Hubbard Brook, *Biogeochemistry*, *60*, 235–316, doi:10.1023/A:1020972100496.

Lorey, P., and C. T. Driscoll (1999), Historical trends of mercury deposition in Adirondack lakes, *Environ. Sci. Technol.*, *33*, 718–722, doi:10.1021/es9800277.

Lovett, G. M., S. S. Nolan, C. T. Driscoll, and T. J. Fahey (1996), Factors regulating throughfall flux in a New Hampshire forested landscape, *Can. J. For. Res.*, *26*, 2134–2144, doi:10.1139/x26-242.

MacAvoy, S. E., and A. J. Bulger (1995), Survival of brook trout (*Salvelinus fontinalis*) embryos and fry in streams of different acid sensitivity in Shenandoah National Park, USA, *Water Air Soil Pollut.*, *85*, 445–450, doi:10.1007/BF00476869.

Maurice, P. A., S. E. Cabaniss, J. Drummond, and E. Ito (2002), Hydrogeochemical controls on the variations in chemical characteristics of natural organic matter at a small freshwater wetland, *Chem. Geol.*, *187*, 59–77, doi:10.1016/S0009-2541(02)00016-5.

McCune, B., and J. B. Grace (2002), *Analysis of Ecological Communities*, MjM Software, Gleneden Beach, Oreg.

McDowell, W. H. (1985), Kinetics and mechanisms of dissolved organic carbon retention in a headwater stream, *Biogeochemistry*, *1*, 329–352, doi:10.1007/BF02187376.

McDowell, W. H., and T. Wood (1984), Podzolization: Soil processes control dissolved organic carbon concentrations in stream water, *Soil Sci.*, *137*, 23–32, doi:10.1097/00010694-198401000-00004.

Meili, M. (1991), The coupling of mercury and organic matter in the biogeochemical cycle: Towards a mechanistic model for the boreal forest zone, *Water Air Soil Pollut.*, *56*, 333–347, doi:10.1007/BF00342281.

Mierle, G., and R. Ingram (1991), The role of humic substances in the mobilization of mercury from watersheds, *Water Air Soil Pollut.*, *56*, 349–357, doi:10.1007/BF00342282.

Miller, E. K., A. Vanarsdale, G. J. Keeler, A. Chalmers, L. Poissant, N. C. Kamman, and R. Brullotte (2005), Estimation and mapping of wet and dry mercury deposition across northeastern North America, *Ecotoxicology*, *14*, 53–70, doi:10.1007/s10646-004-6259-9.

Munson, R. K., and S. A. Gherini (1993), Influence of organic acids on the pH and acid-neutralizing capacity of Adirondack lakes, *Water Resour. Res.*, *29*, 891–899, doi:10.1029/92WR02328.

Munthe, J., R. A. Bodaly, B. A. Branfireun, C. T. Driscoll, C. C. Gilmour, R. Harris, M. Horvat, M. Lucotte, and O. Malm (2007), Recovery of mercury-contaminated fisheries, *Ambio*, *36*, 33–44, doi:10.1579/0044-7447(2007)36[33:ROMF]2.0.CO;2.

Newton, R. M., J. Weintraub, and R. April (1987), The relationship between surface water chemistry and geology in the north branch of the Moose River, *Biogeochemistry*, *3*, 21–35, doi:10.1007/BF02185183.

Palmer, S. M., and C. T. Driscoll (2002), Acidic deposition: Decline in mobilization of toxic aluminium, *Nature*, *417*, 242–243, doi:10.1038/417242a.

Palmer, S. M., C. T. Driscoll, and C. E. Johnson (2004), Long-term trends in soil solution and stream water chemistry at the Hubbard Brook Experimental Forest: Relationship with landscape position, *Biogeochemistry*, *68*, 51–70, doi:10.1023/B:BIOG.0000025741.88474.0d.

Pierce, R. S. (1967), Evidence of overland flow on forested watersheds, in *International Symposium of Forest Hydrology*, edited by W. E. Sopper and H. W. Lull, pp. 247–253, Pergamon, Elmsford, N. Y.

Rea, A. W., S. E. Lindberg, T. Scherbatskoy, and G. J. Keeler (2002), Mercury accumulation in foliage over time in two northern mixed-hardwood forests, *Water Air Soil Pollut.*, *133*, 49–67, doi:10.1023/A:1012919731598.

Schaefer, D. A., C. T. Driscoll, R. Vandreason, and C. P. Yatsko (1990), The episodic acidification of Adirondack lakes during snowmelt, *Water Resour. Res.*, *26*, 1639–1647.

Schafran, G. C., and C. T. Driscoll (1993), Flow path–composition relationships for groundwater entering an acidic lake, *Water Resour. Res.*, *29*, 145–154, doi:10.1029/92WR02064.

Scherbatskoy, T., J. B. Shanley, and G. J. Keeler (1998), Factors controlling mercury transport in an upland forested catchment, *Water Air Soil Pollut.*, *105*, 427–438, doi:10.1023/A:1005053509133.

Schuster, P. F., J. B. Shanley, M. Marvin-Dipasquale, M. M. Reddy, G. R. Aiken, D. A. Roth, H. E. Taylor, D. P. Krabbenhoft, and J. F. DeWild (2008), Mercury and organic carbon dynamics during runoff episodes from a northeastern USA watershed, *Water Air Soil Pollut.*, *187*, 89–108, doi:10.1007/s11270-007-9500-3.

Sebestyen, S. D., E. W. Boyer, J. B. Shanley, C. Kendall, D. H. Doctor, G. R. Aiken, and N. Ohte (2008), Sources, transformations, and hydrological processes that control stream nitrate and dissolved organic matter concentrations during snowmelt in an upland forest, *Water Resour. Res.*, *44*, W12410, doi:10.1029/2008WR006983.

Shanley, J. B., P. F. Schuster, M. M. Reddy, D. A. Roth, H. E. Taylor, and G. R. Aiken (2002), Mercury on the move during snowmelt in Vermont, *Eos Trans. AGU*, *83*(5), 45–48, doi:10.1029/2002EO000031.

Shanley, J. B., N. C. Kamman, T. A. Clair, and A. Chalmers (2005), Physical controls on total and methylmercury concentrations in streams and lakes of the northeastern USA, *Ecotoxicology*, *14*, 125–134, doi:10.1007/s10646-004-6264-z.

Shanley, J. B., et al. (2008), Comparison of total mercury and methylmercury cycling at five sites using the small watershed approach, *Environ. Pollut.*, *154*, 143–154, doi:10.1016/j.envpol.2007.12.031.

Skjelkvale, B. L., J. L. Stoddard, and T. Andersen (2001), Trends in surface water acidification in Europe and North America (1989–1998), *Water Air Soil Pollut.*, *130*, 787–792, doi:10.1023/A:1013806223310.

Skjelkvale, B. L., et al. (2005), Regional scale evidence for improvements in surface water chemistry 1990–2001, *Environ. Pollut.*, *137*, 165–176, doi:10.1016/j.envpol.2004.12.023.

Skyllberg, U., K. Xia, P. R. Bloom, E. A. Nater, and W. F. Bleam (2000), Binding of mercury (II) to reduced sulfur in organic matter along upland-peat soil transects, *J. Environ. Qual.*, *29*, 855–865.

St. Louis, V. L., J. W. M. Rudd, C. A. Kelly, K. G. Beaty, R. J. Flett, and N. T. Roulet (1996), Production and loss of methylmercury and loss of total mercury from boreal forest catchments containing different types of wetlands, *Environ. Sci. Technol.*, *30*, 2719–2729, doi:10.1021/es950856h.

St. Louis, V. L., J. W. M. Rudd, C. A. Kelly, B. D. Hall, K. R. Rolfhus, K. J. Scott, S. E. Lindberg, and W. Dong (2001), Importance of the forest canopy to fluxes of methyl mercury and total mercury to boreal ecosystems, *Environ. Sci. Technol.*, *35*, 3089–3098, doi:10.1021/es001924p.

Stoddard, J. L., et al. (1999), Regional trends in aquatic recovery from acidification in North America and Europe, *Nature*, *401*, 575–578, doi:10.1038/44114.

Stoddard, J. L., J. S. Kahl, F. A. Deviney, D. R. Dewalle, C. T. Driscoll, A. T. Herlihy, J. H. Kellogg, P. S. Murdoch, J. R. Webb, and K. E. Webster (2003), Response of surface water chemistry to the Clean Air Act Amendments of 1990, *Rep. EPA 620/R-03/001*, U.S. Environ. Prot. Agency, Research Triangle Park, N. C.

Sullivan, T. J., J. M. Eilers, B. J. Cosby, and K. B. Vache (1997), Increasing role of nitrogen in the acidification of surface waters in the Adirondack mountains, New York, *Water Air Soil Pollut.*, *95*, 313–336.

United States Environmental Protection Agency (1996), Method 1669: Sampling ambient water for trace metals at EPA water quality criteria levels, *Rep. EPA 821/R-96/008*, Washington, D. C.

Van Sickle, J., J. P. Baker, H. A. Simonin, B. P. Baldigo, W. A. Kretser, and W. E. Sharpe (1996), Episodic acidification of small streams in the northeastern United States: Fish mortality in field bioassays, *Ecol. Appl.*, *6*, 408–421, doi:10.2307/2269379.

Wellington, B. I., and C. T. Driscoll (2004), The episodic acidification of a stream with elevated concentrations of dissolved organic carbon, *Hydrol. Process.*, *18*, 2663–2680, doi:10.1002/hyp.5574.

Wigington, P. J., D. R. DeWalle, P. S. Murdoch, W. A. Kretser, H. A. Simonin, J. Van Sickle, and J. P. Baker (1996), Episodic acidification of small streams in the northeastern United States: Ionic controls of episodes, *Ecol. Appl.*, *6*, 389–407, doi:10.2307/2269378.

Yin, Y. J., H. E. Allen, C. P. Huang, and P. F. Sanders (1997), Interaction of Hg (II) with soil-derived humic substances, *Anal. Chim. Acta*, *341*, 73–82, doi:10.1016/S0003-2670(96)00509-0.

Young, K. C., P. A. Maurice, K. M. Docherty, and S. D. Bridgham (2004), Bacterial degradation of dissolved organic matter from two northern Michigan streams, *Geomicrobiol. J.*, *21*, 521–528, doi:10.1080/01490450490888208.

J. D. Demers, Department of Geological Sciences, University of Michigan, 1100 N. University Ave., Ann Arbor, MI 48109, USA. (jdemers@umich.edu)

C. T. Driscoll, Department of Civil and Environmental Engineering, Syracuse University, Syracuse, NY 13244-1190, USA.

J. B. Shanley, U.S. Geological Survey, PO Box 628, Montpelier, VT 05601, USA.